

Politecnico di Torino



Master's degree in Mechatronic Engineering

Automatic evaluation of the Nine Hole Peg Test for subjects with neurological pathologies through artificial vision approaches

Supervisors:

Prof. Gabriella Olmo

Dr. Roberto Nerino

Dr. Claudia Ferraris

Author:

Sanaa Fariss

September 2020

Abstract

According to the World Health Organization, Cardiovascular Diseases are the first cause of death globally and, among these, stroke is the second one. Stroke is a very serious acute pathological condition, responsible for the appearance of numerous neurological deficits caused by insufficient blood supply to an extensive area of the brain. This event causes cognitive and motor deficits that influence the individual's capacity for autonomy and that hinder self-sufficiency, making the person unable to perform daily life tasks in total independence. The degree of disability that derives from it, beyond gravity, makes the rehabilitation treatment necessary.

Considering the social and economic impact of stroke, monitoring the progress of outpatients in home-based rehabilitation is paramount, because the risk of re-hospitalization can be reduced. A frequent traditional home-based assessment of the disease is not viable because the costs for healthcare system, but other low-cost solutions based on computer vision approaches can be pursued. In this context, one of the most common clinical tests used for the assessment of the upper limb functions and the fine manual dexterity of post-stroke patients is the Nine Hole Peg Test (NHPT).

In this Master Thesis, the post-stroke is considered as a case study, and the focus is on the automated evaluation of the NHPT by a computer vision approach. The movements of the patient's hand are analysed during the performance of the test, both to evaluate the standard time scores of the test, and to provide further information to clinicians about the individual's performance. The system for the automated assessment is based on a hardware made of an RGB-D camera and gloves with coloured markers, and a software which implements computer vision algorithms for the capture and the analysis of the upper limb movement. The software evaluates the completion time for the test and characterizes the movements by a set of kinematic parameters. The software outcomes support both the NHPT standard clinical assessment and the evaluation of the efficacy of the rehabilitation treatments in a home environment.

This work on NHPT is a part of a more extensive study aimed to the overall assessment of motor impairment in the upper limb, which is applicable not only for post-stroke but also in the context of other neurological diseases.

In this thesis work, the performance of the system is experimentally evaluated. Healthy subjects and subjects with mild post stroke side effects are analysed while performing the NHP test. Experimental results show that the system is able to automatically evaluate the standard NHPT scores of both classes of subjects. Furthermore, the kinematic parameters considered are able to capture the differences in the motor performance of the two classes. These preliminary results support the feasibility for an automated assessment of post-stroke patients at home.

keywords

upper limb motor evaluation; stroke; 9 Holes Peg test; automated assessment of disease; hand movement; computer vision techniques, RGB-D camera.

Acknowledgements

I would first like to thank my supervisors Prof. Gabriella Olmo for her constructive suggestions and for providing a pleasurable working atmosphere. I would like to thank dr. Roberto Nerino and dr. Claudia Ferraris for their valuable guidance. This work would not have been realized without their precious advice and their strong support.

I am exceptionally grateful to my friends for supporting me throughout these years and for all the great moments shared together.

Last, but not least, I wish to thank my parents and my brothers and sisters for their love and encouragement throughout my studies.

Contents

<i>Abstract</i>	3
<i>Acknowledgements</i>	4
<i>Introduction</i>	9
1. Stroke	11
1.1 <i>Introduction</i>	11
1.2 <i>Definition of stroke</i>	11
1.3 <i>Signs and symptoms</i>	13
1.4 <i>Stroke risk factors</i>	15
1.4.1 <i>Modifiable risk factors</i>	15
1.4.2 <i>The non-modifiable risk factors</i>	18
2. Clinical evaluation of post-stroke	19
2.1 <i>Introduction</i>	19
2.2 <i>Hand rehabilitation</i>	19
2.3 <i>Reach and Grasp evaluation</i>	20
2.3.1 <i>The Reach Scale (REACH)</i>	20
2.3.2 <i>Box and Blocks Test (BBT)</i>	21
2.3.3 <i>Action Research Arm Test (ARAT)</i>	21
2.4 <i>NIH-Stroke Scale (NIHSS)</i>	21
2.5 <i>Scales for upper extremity evaluation (measures)</i>	22
2.6 <i>Example of evaluation protocol for MESUPES</i>	26
2.7 <i>Nine Hole Peg Test (NHPT)</i>	28
3. Nine-hole peg test	30
3.1 <i>Introduction</i>	30
3.2 <i>Test Procedures and Instructions</i>	30
3.3 <i>The advantages and shortcomings of NHPT</i>	31
3.4 <i>the Standardized Nine Hole Peg test</i>	32
4. Data acquisition system	34
4.1 <i>Introduction</i>	34
4.2 <i>RGB-Depth cameras</i>	34

4.3 Hardware of the acquisition system	36
4.4 Software of the acquisition system	39

5 Computer vision approach for the analysis of the 9 Hole 43

Peg Test

5.1 Introduction.....	43
5.2 Automatic detection and tracking of hand.....	43
5.3 Automatic detection and tracking of board.....	50
5.4 Analysis of colour spaces on tracking robustness.....	51
5.5 Holes detection on the board.....	58
5.6 The management of overlapping bounding boxes.....	64
5.7 Automatic detection of the start and endpoint of the test.....	66
5.7.1 The trajectory of the hand in 2D space.....	67
5.7.2 The trajectory of the hand in 3D space.....	69
5.8 The graph " hand in Movement"	71
5.9 The graph "BB overlapping"	72
5.10 Motion Analysis Results: Kinematic Parameters	73

6 Case Study: Application to Post-Stroke subjects 77

6.1 Introduction	77
6.2 Color Thresholds issue	78
6.3 Board Tracking problem.....	79
6.4 Shadow of the hand on the board	80
6.5 Motion analysis results: Trajectories and graphics.....	81
6.5.1 The trajectory of the hand in 2D space.....	81
6.5.2 The trajectory of the hand in 3D space.....	82
6.5.3 The graph of the holes detected.....	82
6.5.4 The graph " hand in Movement"	83
6.5.5 The graph "BB overlapping"	83
6.6 Motion Analysis Results: Kinematic Parameters	84

7 Conclusion. 87

Bibliography.....	90
-------------------	----

List of Figures

Figure 1.1: CT image showing a case of ischemic stroke (the arrow indicates the ischemic area)

Figure 1.2: CT scan of an intraparenchymal bleed (bottom arrow) with surrounding edema (top arrow)

Figure 1.3: example of Arm drift: Normal: both arms move equally or not at all; Abnormal: one arm drifts

Figure 1.4: Image of a subject with face numb after stroke event

Figure 1.5 :Image of a subject that woke up 19 days later after stroke event unable to walk and talk.

Figure 2.1: Patient while training the hand motor skills

Figure 2.2: The National Institute of Health (NIH) scale

Figure 2.3: The MESUPES _arm section

Figure 2.4: The MESUPES hand section: Range of Motion evaluation

Figure 2.5:The MESUPES arm section

Figure 2.6: The MESUPES stage

Figure 2.7: An example of test kit for NHPT

Figure 3.1: Example of NHPT being administered to a subject

Figure 3.2: The enlarged pegboard shows the standardized order of which peg to pick and which hole to fill, the arrow indicates the direction of the movement.

Figure 4.1: An example of RGB and depth images generated by the device

Figure 4.2: The RGB-Depth Microsoft Kinect v.1 camera is equipped with RGB sensor, an IR depth sensor and an IR projector. From

Figure 4.3: The colored gloves

Figure 4.4: HAND-position and system set-up

Figure 4.5: Activation of the program

Figure 4.6: patient card

Figure 5.1: Original frame (RGB format) of the video sequence (starting position of the hand)

Figure 5.2: The Color Thresholder App

Figure 5.3: The Color Thresholder App was used to identify the hand

Figure 5.4: Color Thresholder automatically sets the image threshold based on the color of the hand

Figure 5.5: image mask obtained with color segmentation procedure

Figure 5.6: Left: Depth Segmentation mask obtained from the first frame; right: the result of color

Figure 5.7: Left: RGB image with the bb mask on the first frame; right: RGB image showing the bounding box of the hand after the application of the Distance Segmentation mask on the first frame

Figure 5.8: Detection of the hand in the first frame. Both the Bounding box and its centroids (2D position on the image) are shown.

Figure 5.9: Detection of two bounding boxes on the hand

Figure 5.10: Example of bounding Box selection when the bwareafilt is used

Figure 5.11: Example of bounding Box selection when the imclose is used.

Figure 5.12: image mask obtained with color segmentation procedure

Figure 5.13: Board detection and tracking

Figure 5.14: Depth image (left) showing image mask applied on the first frame in RGB color space, Depth image (right) showing image mask applied on the first frame in HSV color space.

Figure 5.15: Depth image (left) showing image mask applied on the first frame in RGB color space, Depth image (right) showing image mask applied on the first frame in HSV color space

Figure 5.16: Automatic detection and tracking of hand and board for RGB color space (first frame of the video sequence)

Figure 5.17: Automatic detection and tracking of hand and board for the HSV color space (first frame of the video sequence)

Figure 5.18: Two centroids of the hand in RGB color space (yellow) and in HSV color space on the hand (red)

Figure 5.19: Depth image showing the two centroids of the hand in RGB color space (yellow) and in HSV color space on the hand (red)

Figure 5.20: Color image showing, the two centroids of the hand in RGB color space (yellow color) and in HSV color space on the hand (red color)

Figure 5.21: Depth image showing, the two centroids of the hand in RGB color space (yellow color) and in HSV color space on the hand (red color)

Figure 5.22: Difference between X_{rgb} and X_{hsv} versus time.

Figure 5.23: Difference (in pixel) between Y_{rgb} and Y_{hsv} versus the time.

Figure 5.24 : Left: original image, right: figure shows grayscale image

Figure 5.25: Left: board before applying the morphological filters, right: board after applying the morphological filters.

Figure 5.26: The circular holes detected by the imfindcircles. The circles are displayed using the viscircles function.

Figure 5.27: Example of multiple circles detected for the same hole.

Figure 5.28 : Y axis: the number of holes detected on the board; X axis: the time spent from the starting of the test

Figure 5.29: Correct number of holes after removing multiple circles

Figure 5.30: Correct number of holes detected on the board as function of time.

Figure 5.31: RGB image showing that the test was completed with 6 pegs inserted

Figure 5.32: Board tracking, hand tracking and holes detection (first frame of the video sequence)

Figure 5.33: Left holes detection algorithm is applied; on the center: holes detection algorithm is suspended (bounding boxes partially overlap); Right: holes detection algorithm is resumed.

Figure 5.34: Example of overlapping between the two bounding boxes: the overlapRatio is less than 1 (overlapRatio= 0.0193) denoting a partial overlapping

Figure 5.35: Example of no-overlapping condition between the two bounding boxes: in this case overlapRatio is zero.

Figure 5.36: 2D distance (in pixel) between initial and actual bounding box position of the hand vs time (in seconds) for RGB color space (red) and HSV color space (blue) representation.

Figure 5.37: The same graphs of Fig.5.35 with the RMS error between the two trajectories (green line)

Figure 5.38: The distance between the trajectories of the hand in 3D space vs time, both in the HSV color space (red color) and in RGB color space (blue color) respectively

Figure 5.39: The same graphs of Fig. 5.37 with the RMS error between the two trajectories (green line)

Figure 5.40: “0” corresponds to hand "steady "condition, “1” to hand "moving "condition.

Figure 5.41: “0” corresponds to the non-overlap condition (board occlusion) of hand and board, “1”

Figure 6.1: Two tests performed in different ambient lighting conditions

Figure 6.2:Left: the area of patient’s arm was confused by the board tracking algorithm; Center: image mask; Right: the final image mask obtained.

Figure 6.2 : Final result obtained: the board was detected correctly by the board tracking algorithm.

Figure 6.3: Image mask of first frame.

Figure 6.4: The effect of the shadow of the hand on the image mask

Figure 6.5: Trajectory of the hand in 2D space (in RGB color space) vs. the time (in s).

Figure 6.6: Trajectory of the hand in 3D space vs time, in RGB color space

Figure 6.7: Correct number of holes detected on the board, versus time

Figure 6.8: “0” : "steady hand"; “1”: "moving hand".

Figure 6.9:“0”: no-overlap between hand and board; “1”: overlap between hand and board

List of Acronyms

NHPT: Nine-Hole Peg Test

ARAT: Action Research Arm

BBT: Test Box and Blocks Test

NIHSS: National Institute of Health Stroke Scale

S-NHPT: Standardized Nine Hole Peg test

ADL: Activities of Daily Living

List of Tables

Table 5.1: The thresholds set in the RGB color space.

Table 5.2: The thresholds set in the HSV color space.

Table 5.3: Mean values of the difference between pixel coordinates of the centroids evaluated in RGB and HSV color spaces.

Table 5.4: Mean and standard Deviation , Max and Min values of RMSE (2D space).

Table 5.5: Mean and standard deviation, Max and Min values of RMSE (in 3D space).

Table 5.6: Kinematic Parameters for tracking algorithm in HSV color space.

Table 5.7: Kinematic Parameters in RGB color space.

Table 6.1: The thresholds set in the RGB color space.

Table 6.1.: Kinematic Parameters in RGB color space.

Introduction

The global prevalence of stroke in 2010 was 33 million, with 16.9 million people having a first stroke, of which 795,000 were American and 1.1 million European [1]. It has been estimated that about a third of people they failed to restore upper limb capacity although receiving treatment. This has important consequences for both the individual and the society in general as reduced upper limb function is related with addiction and poor quality of life for both patients and caregivers and effects on national economies.

While stroke has the highest prevalence, other neurological conditions such as multiple sclerosis (MS), spinal cord injuries (SCI) and Brain's traumatic injuries have a significant incidence and there are often similarities in presentation, in the treatment and therefore in the evaluation.

Providing evidence-based and profitable rehabilitation of the upper limbs is a priority for patients and healthcare services and is increasingly important due to the growth of new technology-based interventions designed to improve conventional occupational physical therapy [1].

The Nine Hole Peg Test is a frequently used task in many clinical populations by occupational therapists as a quick measurement of finger dexterity, where the only outcome variable is the time taken to complete the test. this test uses a wide range of functional hand activities to evaluate dexterity; a relatively inexpensive construction cost and short administration times can justify its widespread use.

The focus of this thesis work is to find the most suitable model structure to analyse this test. It involves Computer Vision techniques to analyse the sequence of colour and depth images of the test, captured by RGB-Depth camera.

In this Thesis, the focus is the automatic evaluation of NHPT through kinematic parameters able to characterize the movement performed and support the clinical evaluation, especially with a view to quantitatively assess the effectiveness of a rehabilitation treatment and to use these tools in remote monitoring and rehabilitation applications in the domestic environment.

The remaining part of the document is structured as follows:

Chapter 1 introduces the general characteristics of Stroke.

In chapter 2 clinical evaluation of post-stroke is presented.

In chapter 3 the Nine Hole Peg Test is described.

Chapter 4 describes the methods that have been used for analysing the nine-hole peg test.

Chapter 5 describes the analysis procedure used for an automatic test evaluation; results analysis of the movement (for healthy subject) are presented.

Chapter 6 describes the movement analysis results (for post stroke subject) and comparison with the healthy subjects.

CHAPTER 1

stroke

1.1 Introduction

Annually, 17 million people worldwide suffer a stroke. Of these, 5 million die and another 5 million are left permanently disabled, placing a burden on family and community [2]. In the United States stroke is the second leading cause of death and the leading cause of disability. In Italy stroke is the third leading cause of death after cardiovascular disease and cancer, causing 10% -12% of all deaths, and represents the main cause of invalidity [3].

The stroke prevalence rate in the elderly Italian population (age 65-84 years) is 6.5%, higher in men (7.4%) compared to women (5.9%), and progressively increases with age, reaching the maximum frequency, particularly in the over-85-year-olds. 75% of strokes occur in people over 65 [4]

Ischemic stroke represents the most frequent form of cerebral ischemic event (about 80%), while intraparenchymal hemorrhages affect 15% -20% of cases and subarachnoid hemorrhages about 3%. Ischemic stroke affects individuals with an average age of over 70 years, more often men than women; intraparenchymal hemorrhagic disease affects older subjects, with a slight prevalence for men; Subarachnoid hemorrhage most often affects middle-aged female subjects [4]

Based on the findings of The Burden of Stroke in Europe report, conducted in 2015 by the Stroke Alliance for Europe, the prevalence and the incidence of stroke in Italy were about 300 and 53 strokes per 100.000 inhabitants respectively, of which 80% are new, 20% relapses [5].

In this chapter the main features of stroke are presented, signs and symptoms of stroke will be described, and stroke risk factors will be presented.

1.2 Definition of stroke

In the 1970s the World Health Organization defined stroke as a "neurological deficit of cerebrovascular cause that persists beyond 24 hours or is interrupted by death within 24 hours" [6]

Stroke is a medical condition in which poor blood flow to the brain results in cell death. There are two main types of stroke [2]

Ischemic: It is an interruption of blood flow to the brain due to the occlusion of an artery, which causes an insufficient transport of oxygen and nutrients to that organ, followed by the death of its cells. This condition can cause a symptomatology that depends on the type of vessel affected and the involved portion of the brain.



Figure 1.1: CT image showing a case of ischemic stroke (the arrow indicates the ischemic area) [7]

- **Haemorrhagic:** it is caused by the rupture of a blood vessel in or on the surface of the brain, with bleeding into the surrounding tissue.



Figure 1.2 CT scan of an intraparenchymal bleed (bottom arrow) with surrounding edema (top arrow) [8]

In both cases, the areas of the brain damaged by the event do not work properly. As a consequence, the parts of the body linked to these brain areas and functions are compromised. In particular, if the ischemic or haemorrhagic event concerns areas in the right hemisphere of the brain, the body function impairment will affect the left side of the body; if the event affects areas on the left hemisphere of the brain, the impairment will affect the right side of the body.

1.3 Signs and symptoms

Signs and symptoms often develop quickly, but they can also occur over hours or even days. The typical symptoms of stroke depend on the type and area of the brain affected; they generally manifest with:

- sudden weakness;
- paralysis (impossible movements) or numbness of face, arms or legs, especially on one side of the body;
- confusion;
- difficulty in speaking or understanding language;
- disturbances in the sight of one or both eyes;
- respiratory problems;
- dizziness, trouble in walking, loss of balance or coordination, sudden falls;
- loss of consciousness;
- sudden and intense headache;

Duration and severity of the manifestations vary from one patient to another. The following figures show some typical conditions after the stroke event. In figure 1.3, the “drift of the arm” is verified by this simple test performed with the eyes closed and the arms outstretched: in normal conditions, both arms move in the same way or do not move; in abnormal conditions, such as after stroke, one of the arms (opposite the damaged brain area) may fall down denoting an impairment of the motor control.



Figure 1.3 example of Arm drift: Normal: both arms move equally or not at all; Abnormal: one arm drifts [9]



Figure 1.4 Image of a subject with face numb after stroke event [10]

Face numbing is a common event in stroke (figure 1.4). The following figure 1.5 show a 23-year-old subject who suffered a massive aneurysm rupture causing a stroke. His brain haemorrhage was so severe, that he was placed in a medically induced coma and underwent a craniectomy to reduce the brain swelling. He woke up 19 days later unable to walk and talk.



Figure 1.5 Image of a subject that woke up 19 days later after stroke event unable to walk and talk [11]

To increase the chances of a functional recovery of the injured body part, it is essential that therapies and treatments are started as soon as possible, even during the hospitalization period following the post-acute phase .

Every minute in which a large vessel ischemic stroke is untreated, the average patient loses 1.9 million neurons, 13.8 billion synapses, and 12 km (7 miles) of axonal fibres. Each hour in which treatment fails to occur, the brain loses as many neurons as it does in almost 3.6 years of normal aging [12].

1.4 Stroke risk factors [13]

1.4.1 Modifiable risk factors

There are factors that can increase the risk of having a stroke. These factors include hypertension, diabetes, overweight (obesity), hypercholesterolaemia, sedentary lifestyle, smoking and alcohol abuse. These factors are defined "modifiable" as they can be corrected through lifestyle changes, or through appropriate drug therapy [5]

Hypertension

Hypertension is a chronic condition characterized by a stable increase in blood pressure in the arteries [14]

A certain level of blood pressure is necessary for the blood to flow throughout the circulatory system, ensuring the necessary nourishment to the body's tissues. The heart beats regularly and in this way pumps blood into the arteries: the force exerted by the blood flow against the walls of the vessels is blood pressure

The moment when the pressure reaches the highest value corresponds to the contraction phase of the heart (called "systole") and is called "maximum (or systolic) pressure". The moment when the pressure is lowest corresponds to the relaxation phase of the heart and is defined as "minimum (or diastolic) pressure".

The pressure with which blood flows into the arteries increases if the walls of these vessels harden and lose their elasticity, narrow in diameter or become blocked. In these cases, the heart must pump harder to oppose the increase in resistance that hinders blood flow and to ensure that the blood irrigated all the tissues of the body, avoiding phenomena of "ischemia", i.e. situations in which not enough oxygen reaches the tissues for a deficit in the blood supply .

Hypertension is a "silent enemy", because if it does not produce obvious damage to organs, there are no symptoms that signals its presence. Today, in fact, many people are affected by hypertension and do not know they are. It is therefore important to regularly check blood pressure, also because if properly treated, it stops representing a danger to our health. In any case, it is essential to always contact the doctor, who will offer the patient the safest and most suitable drug therapy for the individual case [15] .

Diabetes

Diabetes is a disease in which blood glucose levels are constantly above normal values (126 mg / dl). In Italy 9% of men and 6% of women are diabetic, while 9% of men and 5% of women are in a risky condition, with blood glucose values between 110 and 125 mg / dl [16] .

Over time, diabetes leads to changes in the walls of the blood vessels, both in the larger arteries and in the capillaries, with a consequent increase in the risk of stroke [17].

Type 1 diabetes is characterized by deficient insulin production and requires daily administration of insulin

Type 2 diabetes is the most frequent one and occurs in adulthood; it and often depends on excess weight, and diet is the best preventive weapon. A balanced diet that is not too rich in sugars, together with the control of body weight and blood sugar (just a simple blood test) allows to keep the danger away.

Overweight

Excess weight increases the combined risk of high cholesterol and diabetes. In fact, those who tend to gain weight also easily have a very rich diet and are therefore more at risk of having high cholesterol and blood sugar levels. Having total blood cholesterol above 240 mg / dl or good HDL cholesterol below 35 mg / dl increases the risk of stroke. In Italy 21% of men and 25% of women have a total cholesterol value equal to or greater than 240 mg / dl [18].

36% of men and 33% of women are in a risk condition with cholesterol between 200 and 239 mg / dl. An excessively high diet of animal fats (milk derivatives, fatty meats, salami ...) is linked to an increase in cholesterol in the blood, in particular of the "bad" cholesterol (LDL cholesterol), which tends to remain in the vessels and therefore facilitates atherosclerotic plaques along the arteries.

Sedentary lifestyle

Sedentary lifestyle is primarily linked to weight gain and therefore to the possibility of obesity and diabetes. It promotes the onset of hypertension and increases "bad" cholesterol levels (linked to lipoproteins, LDL). In Italy 34% of men and 46% of women do not perform any physical activity during free time.

Smoke

Smoking is a fearsome enemy of blood vessels. Every time a cigarette is sucked, nicotine is absorbed by the lungs, then it passes into the circulating blood and up to the brain, with different, but all negative consequences:

- platelet aggregation increases (the tendency of platelets to attach to each other and form clots in the arteries)
- increased blood pressure.

A further negative effect is on the activity of the endothelium of the arterial vessels, of which smoking prevents normal functioning: this leads to atherosclerosis, which is closely related to stroke. In the Italian population, the habit of cigarette smoking effects on average 30% of men and 21% of women [19].

Atrial fibrillation

Atrial fibrillation is an arrhythmia leading to an alteration of the normal heartbeat. If not diagnosed, therefore without the protection offered by adequate oral anticoagulant therapy, it represents an important risk factor for stroke. This is the most common heart rhythm anomaly in the adult population and affects about 1,000,000 people in Italy, with 120,000 new cases every year [20]. This refers only to the ascertained cases, but the total ones are much more numerous because many people who suffer from them do not present disturbances and are unaware that they have this problem.

Asymptomatic atrial fibrillation is particularly dangerous because the person suffering from it is not aware of its presence, and therefore is not subjected to the appropriate therapies, with the consequent considerable increase in the risk of stroke.

The risk of atrial fibrillation increases with age: 1 in 4 people, over 40 years of age, present elements of risk due to its appearance. Atrial fibrillation and its consequences can be kept under control especially if diagnosed in time.

1.4.2. The non-modifiable risk factors

Age is the major non-modifiable risk factor for stroke. The incidence of the cerebrovascular event increases with age and from the age of 55 it doubles for each decade. Most strokes occur after the age of 65. In addition, belonging to the male gender and family predisposition are additional risk factors that cannot be modified for the occurrence of stroke.

CHAPTER 2

Clinical evaluation of post-stroke

2.1 Introduction

Motor impairment is a common problem for people affected by neurological disabilities, with a negative impact on daily activities, motor performance, independence and more in general, the quality of life. Partial or total impairment of the motor functions is the typical consequence of stroke events that cause more or less severe forms of hemiparesis or hemiplegia of one side of the body. Accurate and timely evaluation of the impairment severity is needed for effective rehabilitation treatments and therapies, and for the development of new intervention strategies for the partial or complete recovery of the injured body part [21]

The assessments of the motor impairment are generally conducted by a healthcare professional, with experience in the use of the several standard measurement scales and should include not only the evaluation of motors functions and body structure, but also activity and participation.

The functional recovery of the upper and lower limbs is significantly different: in fact, the grosser motor function of the lower limbs recovers faster than upper limbs, in particular the finer movement of the hands.

Functional recovery takes place through appropriate rehabilitation paths, adapted to the level of impairment of the affected functionality. The "traditional" post-stroke rehabilitation treatment aims at recovering the motor function of the compromised part of the body (in general hemiparesis) through the relearning of primary functional skills that restore autonomy and independence to the person in everyday life. The continuation of the treatment in a home context, through adequate and continuous stimulation, allows on one hand to improve / maintain the reacquired functionality over time, but also to avoid the "learned non-use" phenomenon caused by the voluntary "non-use" of the rehabilitated limb which inevitably leads to functional deterioration.

In the context of this thesis, attention was focused on the motor aspects of the upper limb, in particular the hand, with the aim of reaching an objective and automatic evaluation of the motor function to be used, in the near future, in home rehabilitation.

2.2 Hand rehabilitation

Hand is one of the most important structures of human body. The hands can not only complete many gross motor skills but also engage in various sophisticated and fine activities that are closely related

to daily life. Rehabilitation of the hand function has become a challenge and hotspot of modern rehabilitation medicine research [22]

Rehabilitation and training programs can effectively wake up the residual function of neurons to participate in activities, so as to contribute to the recovery and reconstruction of sensory feedback, prompting constantly modification of the quality of the action via the central nervous system . Rehabilitation eventually results in the recovery of the original function or the establishment of a new area of compensation, to achieve functional remodelling and to improve the skills of the body.

The human hands are very complex and versatile. Research shows that the relationship between the distal function of the upper limb (i.e., the hand) and the ability to perform activities of daily living (ADL) is stronger than in the other limbs. The deficit in hand function have a severe impact on patients' quality of life, which means that more demand is needed on hand motor recovery.

An example of exercise to practice and train the motor skills of the upper limbs and hands in shown in figure 2.1.



Figure 2.1 Patient while training the hand motor skills [23]

2.3 Reach and Grasp evaluation

Reaching and grasping actions are two examples of habitual movements in daily life that are commonly compromised after stroke ,so that the functional independence of individuals is directly influenced by the ability to perform reaching and grasping movements properly. The execution of these activities is severely affected as consequence of the brain damage, leading to slower and fragmented movements that ,in turn, can be linked to compensatory movements by other body structures , in particular shoulders and trunk [24].

2.3.1 The Reach Scale (REACH)

The Rating of Everyday Arm-use in the community and home (REACH) scale [25] focuses on compensatory strategies that are used during the transport phase in the range of motion and is defined by time from the beginning of the movement until the object is reached

2.3.2 Box and Blocks Test (BBT)

The Box and Blocks Test (BBT) consists of a manual dexterity test where a wooden box is used, divided in two parts by a partition higher than the edges of the box [26]. Evaluation occurs by the number of wooden cubes (2.5 cm) carried from side to side of the box for 1 min. The test is performed primarily with the unaffected limb, followed by the compromised limb.

2.3.3 Action Research Arm Test (ARAT)

Finally, the ARAT, also known as the Upper Limb Extremity Action Test, has 19 items that evaluate complex grip-related UE activities [27]. The total score ranges from 0 (no movement can be performed) to 57 (normal motor performance).

Action Research Arm Test (ARAT) aims to quantify movement changes through observational analyses, further classified on either ordinal or nominal scales,

2.4 NIH-Stroke Scale (NIHSS)

A patient can be assessed using an evaluation scale, called NIHSS [28], of which an Italian version exists, edited by the Department of Neurological Sciences of Sapienza in Rome and by the Public Health Agency of the Lazio region in 2003. The certification of correct use of the scale is obtained by passing the simulated patient assessment test.

The National Institute of Health (NIH) stroke scale (Figure 2.2) is universally used in daily clinical practice and research to quantify the severity of the neurological deficit caused by an acute brain stroke. It consists of 11 items and the total score ranges from a minimum of 0 = normal neurological examination to a maximum of 42, severe neuro-sensory-motor deficit

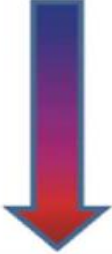
NIHSS SCORE	STROKE SEVERITY	IMPACTED BRAIN DENSITY
0	No Stroke	
0 – 4	Minor Stroke	
5 – 15	Moderate Stroke	
16– 20	Moderate to Severe Stroke	
21 - 42	Severe Stroke	

Figure2.2: The National Institute of Health (NIH) scale

The score gives us an idea about the patient's clinical status and, in a certain sense, about the severity of the signs and prognosis.

The NIH stroke score > 22 is considered to be very significant and may indicate an increased risk of complications. Scoring is normally used to track the outcome, improvement or deterioration of a stroke.

One of the limitations of NIHSS is the poor assessment ability about consciousness and dysarthria; moreover, it investigates little the cranial nerves and has low sensitivity and specificity as a test for cerebellar and trunk lesions.

Severity of a stroke is heavily correlated with the volume of brain affected by the stroke; strokes affecting larger portions of the brain tend to have more detrimental effects [29]. NIHSS scores have been found to be reliable predictors of damaged brain volume, with a smaller NIHSS score indicating a smaller lesion volume [30]. An example of the application of NIHS to prediction and in-depth analysis of stroke severity of elderly over 65 years is presented in [31]

2.5 Scales for upper extremity evaluation (measures).

The clinical scales that evaluate arm function after stroke are generally weak in detecting the quality of movement. To overcome this limitation, a new scale has been developed to evaluate and roughly quantify arm and hand movements, generating a score of the upper limb dexterity of complex functions.

The aim of the MESUPES scale is to measure the quality of the motor function of the hemiparetic arm and hand in stroke patients while performing specific motor tasks related to dexterity, complex functions and movements with arm, hand and fingers [32]

MESUPES-ARM provides the assignment of a score for each exercise in three different conditions: passive, assisted and alone (by himself / herself). In the “passive” mode it is the therapist who makes the movement (the patient is totally passive, and not collaborate with the movement), in the “assisted” mode the therapist makes the movement but the patient collaborates in the movement; in the “alone” mode the patient is able to perform the movement alone. Obviously, this depends on the severity of the motor impairment. A score (0..5) is then assigned based on how it was possible to perform the movement (an X corresponding to the execution mode). In the MESUPES-HAND, the patient performs the movements alone.

The first section of the MESUPES scale concerns the arm movements (Figure 2.3) and consists of 8 motor tasks performed in supine position (tasks 1 to 4) or in sitting position (tasks 5 to 8). The motor tasks are performed by the patient with an active aid of the therapist (passive or assisted mode), or without the aid of the therapist.

The therapist assigns a score to the task execution as indicated by the evaluation criteria of the scale. The maximum achievable score for MESUPES is 58 (MESUPES-Arm maximum score is 40; MESUPES-Hand maximum score is 18) [33].

- Mesupes -arm

MESUPES-arm		EXECUTION					
		passive	assisted	by him/herself			
ITEMS	SCORES	0	1	2	3	4	5
<i>STARTING POSITION</i> supine on a treatment plinth, the head resting on a pillow, a small cylindrical pillow placed under the knees to support the legs, arms extended and resting on the table, forearms in pronation, fingers in a relaxed extended and adducted position							
1. hand to stomach							
2. hand back to the starting position							
3. abduction 0°-90°, arm extended, forearm in neutral position (arm slides on the table)							
4. arm back to the starting position							
<i>STARTING POSITION</i> sitting on a treatment plinth, hips and knees in 90° flexion, feet flat on the floor, forearms rest in 90° elbow flexion and pronation on a table in front of the patient, fingers in a relaxed extended and adducted position							
5. hand from knee (<i>starting position</i>) onto the table							
6. hand(palm) to mouth (elbow remains on the table)							
7. reach with correct orientation of fingers and wrist (as if to grasp) for a plastic bottle (cylinder; diameter 6 cm) standing on the table at arm's length in front of the patient's midline (trunk remains in the same position; grasping the bottle is not required)							
8. hand on top of the head (shoulder in abduction)							
TOTAL							/40

Figure 2.3: The MESUPES _arm section

The score assigned by the therapist to each task depends on the execution mode and on the quality of the movement performed as follows [34].

Passive Mode (scores:0-1)

- the patient is asked to let the therapist perform the movement with the affected arm
- the therapist performs the task slowly to evaluate the adaptation of the tone to the movement
 - 0 = no adequate adaptation of tone to the movement (hyper-or hypotonia)
 - 1 = adequate adaptation of tone (normal tone) to at least part of the movement

Assisted Mode (scores: 2)

- the patient is asked to help performing the movement
- the therapist -assists the patient as much as needed to perform the movement normally
 - feels if and how much the patient actively contributes to the movement in a normal way
- 2 = participation through normal muscle contraction in at least part of the movement

By him/herself Mode (scores: 3-5)

→ the patient performs the movement without help

→ the therapist controls visually how far the patient can move in a normal way

3 = performs part of the whole movement normally

4 = completes the whole movement normally but performs it slowly or with great effort

5 = completes the whole movement normally at normal speed

The second section of the MESUPES scale concerns the hand movements and dexterity, divided into Range of Motion (Figure 2.4) and Orientation (figure 2.5). The maximum assignable score is 18, divided into 12 for the Range of Motion and 6 for the Orientation.

The Range of Motion block consists of 6 motor tasks performed with fingers in sitting position with a table as a support.

The motor tasks are performed by the patient without the aid of the therapist. However, the therapist assigns a score to the task execution as indicated by the evaluation criteria of the scale.

MESUPES-hand

A. Range of Motion

ITEMS	SCORES	EXECUTION		
		0	1	2
<i>STARTING POSITION</i> sitting on a treatment plinth, hips and knees in 90° flexion, feet flat on the floor, forearms rest in 90° elbow flexion and pronation on a table in front of the patient, fingers in a relaxed extended and adducted position				
1. pinch grip (<i>starting position</i> with abduction of thumb; <i>movement</i> : opposition thumb and index; thumb and index remain in contact with the table; take the shortest distance of thumb and index finger movements into account for scoring)				
2. wrist extension (do not allow hyperextension of the fingers; measure distance vertically from hand palm to table at the MCP-joint of the thumb)				
3. opposition thumb and little finger (<i>starting position</i> : reposition (abduction) of thumb; <i>movement</i> : thumb and little finger remain in contact with the table; take the shortest distance of thumb and little finger movements into account for scoring)				
4. selective extension of 3 rd finger				
5. starting position with fingers 4 and 5 slightly spread out; spread index and middle finger simultaneously, sliding on the table (measure distance between fingertips 2 and 3)				
6. selective extension of 5 th finger				
TOTAL				/12

Figure 2.4: The MESUPES hand section: Range of Motion evaluation

The score assigned by the therapist to each task depend on the amplitude of the movement performed, as follows

→ the patient performs the movement without help

→ the therapist controls visually whether and how far the patient can PERFORM THE MOVEMENT in a normal way

0 = no movement

1 = movement amplitude < 2 cm

2 = movement amplitude ≥ 2 cm

The Orientation block (Figure 2.5) consists of 3 motor tasks performed with fingers in sitting position with a table as a support. In this case the patient has to interact with particular objects such as little bottle and to perform more complex actions. Also in this case, the motor tasks are performed by the patient without the aid of the therapist. However, the therapist assigns a score to the task execution as indicated by the evaluation criteria of the scale.

B. Orientation		EXECUTION active		
ITEMS	SCORES	0	1	2
<p><i>STARTING POSITION</i> sitting on a treatment plinth, hips and knees in 90° flexion, feet on the ground, forearms rest in 90° elbow flexion and pronation on a table in front of the patient, abducted thumb and extended adducted fingers are relaxed</p> <p>The therapist places every object in the middle of an imaginary line connecting the distal joints of thumb and index finger</p>				
7. grip plastic bottle (cylinder, diameter 2.5 cm; height 8 cm) with tips of thumb and index finger and lift it 2 cm (forearm remains on the table)				
8. grip dice (1.5 x 1.5 cm) sideways with tips of thumb and index finger and rotate dice once around its vertical axis (keep the dice on the table)				
9. put tip of index finger on the dice and rotate dice once around its vertical axis with fingers 1 and 3 (keep the dice on the table)				
TOTAL				/6

Figure 2.5: The MESUPES arm section

The score assigned by the therapist to each task depends on the quality, in terms of finger position and wrist orientation of the movement performed, as follows

→ the patient performs the movement without help

→ the therapist controls visually whether the patient can ORIENT one or more segments of the arm throughout the movement in a normal way

0 = no movement or movement with abnormal orientation of fingers and wrist towards the object

1 = movement with normal orientation of fingers or wrist towards the object

2 = whole movement correct

The total scores of the MESUPES scale is summarized in the following schema.

Arm items total = /40	Hand items total= /18	TOTAL = /58
-----------------------	-----------------------	-------------

In the scale, a lot of attention is paid to performing "normal" movements. In most cases, the movement can be compared to the contralateral side. In the presence of a pathology that interferes on that side, the movement is compared with what is accepted as a normal movement which means: painless, without tremor, performed with a normal range of movement using adequate muscle contraction and normal orientation of the various bodies' segments. No score is given when performance is based on inadequate adaptation to tone, abnormal, synergistic (twitching / extensor) muscle contractions or massive movement patterns.

The MESUPES arm and the MESUPES hand satisfy the statistical properties of reliability, validity and one-dimensionality. Both tests provide a useful clinical and research tool to qualitatively evaluate the function of the arm and hand during the recovery of the motor function after stroke. [35]

2.6 Example of evaluation protocol for MESUPES.

The evaluation protocol for MESUPES is performed according the following steps [34]:

A) As previously mentioned, the scale is divided in MESUPES-arm and MESUPES-hand. For each subset, a specific starting position is described by the scale. If a patient cannot sit without support, the patient is provided support in the back using a cube cushion. If a patient is still unable to remain in this normally supported sitting position, the related tasks cannot be evaluated. In this case, no score is awarded. After each trial, the therapist helps to reposition the upper extremity to the initial position: The test proceeds the next trial or task only when the muscle tone is normalized again. If a relaxed starting position cannot be achieved, e.g. due to extreme hypertonia, the therapist assigns 0 to that task.

B) Before starting each task, the patient must be meticulously instructed through the following steps:

- ✓ the activity is explained verbally and is demonstrated to make the commands more comprehensible.
- ✓ the patient is asked to perform the activity first with the side not involved, to ensure that the activity is well understood.

C) each task is repeated with a maximum of 3 attempts if the patient performs the activity inadequately and the patient is made aware of the anomalous components of the movement. The movements are considered to be performed normally if no compensation is visible in any other part of the bod (for example: extra movement of the trunk,)

D) Tasks of the **MESUPES-arm** are performed in three consecutive stages (Figure 2.6):

- ❖ phase 1: the activity is executed passively (scores 0-1),

- ❖ phase 2: the therapist assists the patient during the movement (score 2),
- ❖ phase 3: the patient performs the task alone (scores 3-5).

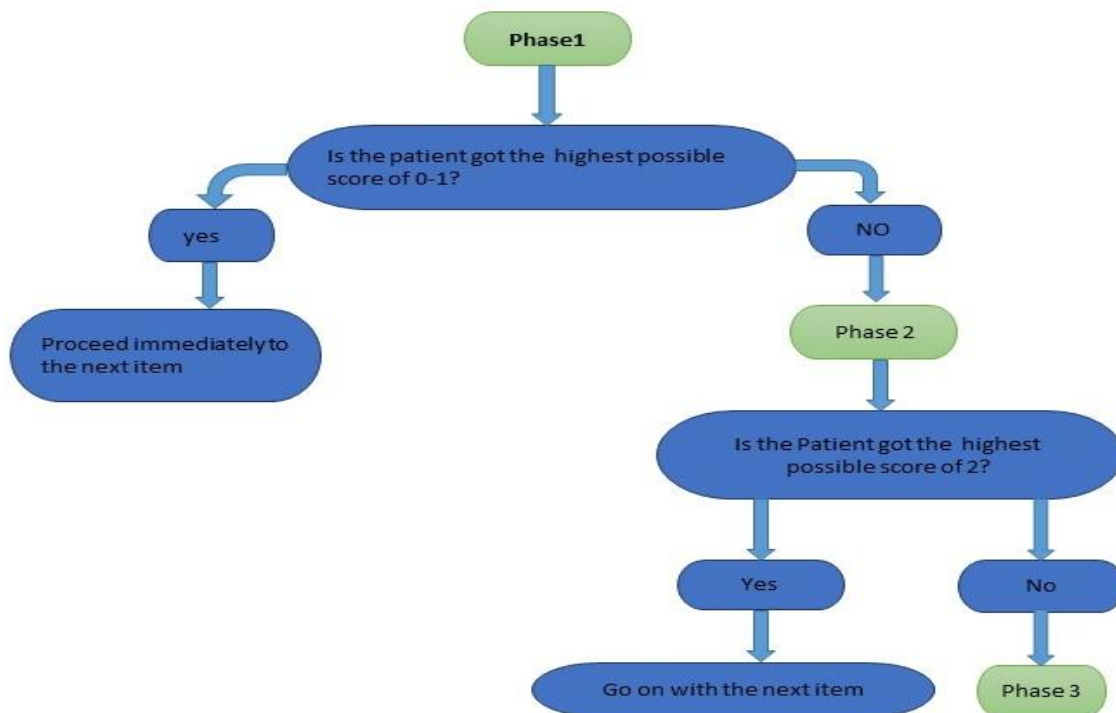


Figure 2.6: The MESUPES stages

Scoring and testing must be done by the same therapist. For each activity, only one score is assigned, which is the highest score that the patient obtains during the test item. The highest score is assigned according to the following evaluation criteria:

Scores 0-1

0= because no adequate adaptation of tone to the movement (abnormal tone: hyper- or hypotonia).

- It is not possible to achieve a relaxed starting position, e.g. due to extreme hypertonia or pain
- A relaxed starting position can be achieved but the arm cannot be moved, e.g. because of the pain
- The tone immediately increases during passive movement (extreme hypertonicity)
- The entire weight of the patient's arm must be supported by the therapist ("floppy" arm - extreme hypotonia)

1= adequate adaptation of the tone (normal tone) to at least part of the movement

- The tone increased only in part of the passive movement

- There is a limited range of motion, e.g. because of pain, but a normalised tone within the limited range of motion
- Normal tone for the full range of passive movement

Scores 2

2= participation through normal muscle contraction in at least part of the movement. When the patient can perform the movement but not in a normal way, you evaluate the quality of movement with the arm supported.

Scores 3-5

3= normally performs part of the whole movement

4= normally completes all movement but performs it slowly or with great effort

5= completes the whole movement normally at normal speed Only that part of the movement is classified as "normal" in which each joint, necessary to perform the movement, participates in a normal way and each muscle tone is normal.

E) In MESUPES-hand, the patient performs all the tasks alone.

In the Range of the Motion tasks, the "amplitude of movement" is estimated by the therapist. The "absolute" value of the distance reached during the movement is evaluated individually and the score is assigned without comparing the performance with the contralateral (the healthy hand). In general, a block of wood that marks 1 and 2 cm or two separate wooden sticks (1 cm and 2 cm) are used during the tasks to approximately estimate the amplitude of the movement.

In the Orientation tasks based on "joint orientation" during the exercise, the score to the performance of the impaired hand is assigned with respect to a performance with normal orientation; As previously mentioned the motor performance is not evaluated with respect to the "healthy side" but to the "normal" performance.

2.7 Nine Hole Peg Test (NHPT)

NHPT [34] a short and quantitative standardized test for the evaluation of the upper limb motor function. It is one of the most common tests for the assessment of finger dexterity. NHPT consists in collecting 9 small pegs and insert them into as many holes of wood or plastic board. Several protocols may be used to evaluate the test. In some protocols, once the insertion is complete, the test is also considered as completed. In other cases, once the insertion is complete, the patient is asked to put away the pegs in the shortest possible time (Figure 2.7).

Otherwise, a maximum time is set to complete the task. Sometimes both the dominant and non-dominant are tested twice. In general, the NHPT is widely used because it is a timed test, with good reliability and good validity.

The thesis has been focused on the automatic evaluation of the NHPT, so a more detailed description of the NHPT will be provided in the next chapter.



Figure 2.7: An example of test kit for NHPT [36]

CHAPTER 3

The Nine Hole Peg Test

3.1 Introduction

Impaired upper limb dexterity is evident in approximately 45-70% of stroke victims one year after stroke. This impairment is often evaluated in clinics by performing the Nine Hole Peg Test (NHPT) [34], which is a dexterity task frequently used in many clinical populations. The test is performed as quickly as possible and the only result variable is the total time to complete the activity. As a result, motor performance is not currently analysed during NHPT although it potentially provides useful information on upper limb dexterity, especially among people with neurological dysfunctions

The Nine Hole Peg Test has been recommended as a clinical test for post-stroke individuals, designed to test and evolve an individual's motor skills or help diagnose neurocognitive disorders. It is a standardized, quantitative test of upper extremity function. From a clinical viewpoint the test is simple and easy to use for both the operator and the patient, showing immediate results regarding the patient's ability to dexterity.

3.2 Test Procedures and Instructions

The Nine Hole Peg Test consists of a board with 9 holes and 9 small pegs. The experimental procedure normally requires that the name, age, sex, hand dominance and occupation of the subject are recorded. Hand dominance is determined by standard question as for example "Are you right-handed or left-handed?". If the subject reported using both hands in the same way, the hand used to write could be considered as the "dominant" hand, as occurs for example in [34] .

The patient is seated at a table with the test kit (consisting of board and pegs) placed on the table and centred in front of him/her (figure 3.1) .The nine pegs are placed on the table next to the board on the same side of the hand with which the test will be performed. The therapist which supervises the test execution, uses a stopwatch to measure the time necessary to complete the test. When the stopwatch is started, the patient begins to collect the nine pegs, one at a time, as quickly as possible and puts them in the board holes in any order until all the holes are filled. In many experimental protocols, the test ends when all the pegs are correctly placed into the board. In other experimental protocols, a maximum time to complete the test is fixed and the number of pegs correctly placed into the board holes is considered to evaluate the performance. In other cases, once all the pegs are in the holes, the patient is asked to remove them as quickly as possible, one at a time, bringing them to the

initial position. In this case the total time to complete both the activities is considered to evaluate the performance. Generally, the test is performed only once, first with the healthy hand and then with the impaired one. In other cases, both the dominant and non-dominant hands are tested twice, with the dominant hand tested first. However, the experimental protocols must define precisely: the instrument to be used (the type of board), the initial setting (where the board and the pins are placed with respect to the patient's position), the questions for the patient (data collection for statistical purposes), the instructions for the patient (what the patient must do), the method of execution (insertion of the pegs only, insertion and removal of the pegs, only compromised hand, both hands, number of executions per hand, maximum time for execution), measurement with stopwatch (when to start and stop the stopwatch), test evaluation criteria (time taken to insert the pegs, total time to insert and remove the pegs, number of pegs in a maximum time).



Figure 3.1 Example of NHPT being administered to a subject [37]

3.3 The advantages and shortcomings of NHPT

The NHPT is a timed test, with good reliability and good validity. The main advantages are simplicity, portability, brevity and sensitivity to changes in hand performance. However, it has some drawbacks, like all the other timed tests: it primarily evaluates the speed with which a task is carried out, but even if the task is performed with a lower speed, the patient may not have performed the assigned task correctly. In practice, the test evaluates only the speed but nothing regarding the quality of the movement performed. In addition, it is also not particularly useful when the patient has a severe impairment in the hand function which causes excessive difficulty in handling very small pegs.

The function of the hand has several subtle variations in movements; it is the sum-total of multi-joint movements, muscle groups with neurological control at various levels. The fusion of all these

physiological factors working in tandem is responsible for the accuracy and effectiveness of hand movement. However, the nine-hole peg test repeatedly classifies the same type of movement. Thus, the subtle recovery of some movements can often be missed simply because they have not been tested in the monotonous repetitive movement that the classification of the NHPT represents [38] .

Despite good general post-stroke test-retest reliability, a low test-retest reliability was found in post-stroke people who have forms of spasticity in the impaired hand which can hinder and limit the correct execution of the test [39].

3.4 the Standardized Nine Hole Peg test

In the NHPT the initial position of the pegs may not be exactly the same and the insertion strategy (order of pin insertion) is not normally indicated: these two elements could therefore affect the time measurement, especially in the case of comparison between repeated evaluations. Several standardized solutions have been proposed. In [39] for example ,the NHPT was modified and standardized (S-NHPT) by 1) replacing the original peg container with another identical nine-hole pegboard, 2) adding a specific order to choose peg and 3) specifying to insert the peg taken from the original pegboard in the corresponding hole of the target pegboard.

In the S-NHPT defined in [39], attempts are no longer allowed if the patient does not follow the specific order. If a peg is dropped on the table or knee, the patient can pick it up. If the peg is dropped on the floor, the patient should continue with the next peg. the S-NHPT must be repeated twice for both hands. Figure 3.2 shows the execution of the S-NHPT.

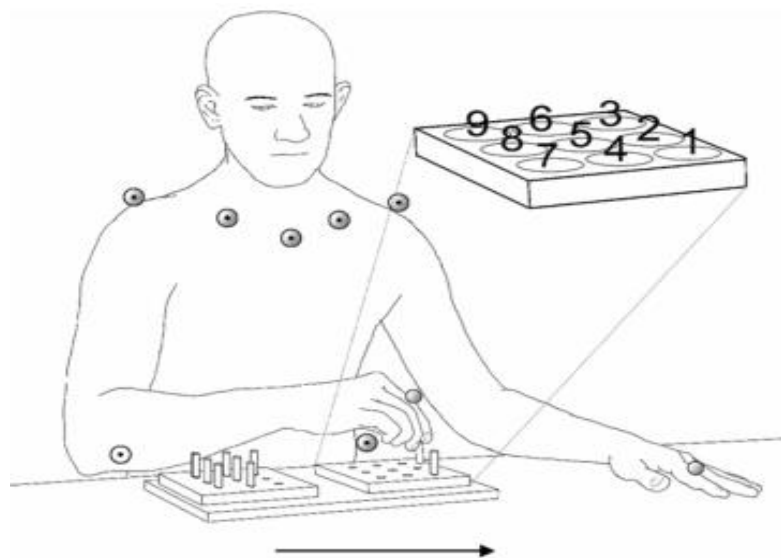


Figure 3.2: The enlarged pegboard shows the standardized order of which peg to pick and which hole to fill, the arrow indicates the direction of the movement.

However, the predefined order about which peg to choose and which hole to fill, may require greater cognitive demands on memory and attention than self-guided performance of the original test. Indeed, some patients were unable to manage the default order of the S-NHPT and this condition could be considered as a drawback in the wide use of the standardized version of the NHPT [39].

Nevertheless, since most daily activities involve cognitive aspects during movements executions, it has been suggested that motor and cognitive aspects should not be assessed or treated separately in people with brain injuries. According to [39], defining the specific order of the pegs in the S-NHPT was justified as it allows to detect interferences between cognition and dexterity that otherwise would not be possible in the NHPT.

A final consideration is that the S-NHPT initially involves collecting pegs already inserted into the board compared to the traditional NHPT, performing gripping actions that requires less fine manipulative control than in case of a pile of mixed pegs, this could be considered as a facilitation in the test execution.

The attempt to standardize the test is important to avoid bias in the results. However, the "constraints" imposed by this "standardized" version (S-NHPT) could be too restrictive for patients with after-effects of stroke, and in particular, the fact of following an insertion order with introduction of significant cognitive aspects into the test and the fact to stop the test if the correct insertion strategy is not followed. A form of standardization can also be defined within the individual case study, through the definition of a clear and precise experimental protocol in order to guarantee repeatability and comparison between different NHPT executions.

CHAPTER 4

Data acquisition system

4.1 Introduction

This chapter describes the acquisition system that has been used for the analysis of the nine-hole peg test (NHPT). The system employs a particular type of depth sensing device that works in association with an RGB camera, constituting a new type of optical device called RGB-Depth camera.

First, a generic RGB-Depth camera is described, with its features and working principles. This camera provides both color (RGB) and distance (DEPTH) information in the form of video streams or image sequences. Second, the details of the acquisition systems are described. Finally, we will see how this system was used to capture the hand performance during the execution of NHPT.

The acquisition system here presented was developed by the Institute of Electronics and Information and Telecommunications Engineering (IEIIT) of the National Research Council (CNR) of Turin , while the video sequences to be analysed were collected at the Neurology and Neurorehabilitation Operative Unit of San Giuseppe Hospital in Piancavallo (VB), a site of the Italian Auxological Institute (IRCSS).

4.2 RGB-Depth cameras

The first consumer RGB-Depth camera was Microsoft Kinect (version 1), developed for the video game market but which found wide space in other fields as robotic, industrial and medical applications.

Next, another version of Microsoft Kinect was released (version 2), and lastly, the most recent one is Microsoft Kinect AZURE. Meanwhile, other companies have released on the market body/hand tracking devices based on depth info, expanding the potential use of these innovative technologies. Some examples are the RGB-Depth cameras ORBBEC Astra, the Intel Realsense family of the devices (415,435, etc.) and the LeapMotion device, based on the real-time stereo reconstruction of IR image pairs of the scene.

The main components of an RGB camera are:

RGB (Color) sensor is the sensor that captures (and produces) the RGB color image. It behaves like a normal webcam; in practice, it captures what is illuminated by "visible" light.

IR sensor is the sensor that captures the IR video stream of the scene illuminated by the IR projector. Depending on the camera type, the projector superimposes an IR dot pattern (triangulation-based

devices) or an amplitude modulated IR light (time-of-flight devices) to the natural IR scene luminance. The dot patterns in the IR video streams are used to recover by triangulation a pixel-by-pixel depth information through a real-time processing. The modulated IR light of the projector reflected from the scene and returning to the IR sensor is demodulated to recover the distance of the points in the scene. The IR camera can capture what is illuminated by the IR light, not visible to the eye. This is a big advantage because the projected light doesn't disturb the subjects and it can operate also in a dark environment.

IR projector: infrared (IR) light which project on the scene an IR dot pattern.

Due to the different positions of the color camera depth sensor, their images are slightly shifted one compared to the other, and they need to be realigned (or registered) to have correct pixel-by-pixel correspondence between IR and RGB images.

RGB and DEPTH images

In the RGB image, each pixel is associated to a triple (corresponding to the intensity of R, G, B channels) which together determine the color of a point. A depth images is a 2D pixel map where every pixel is associated to a line of view and to a corresponding 3D point in the scene. The distance between this 3D point and the IR sensor corresponds to the pixel value of the depth map.

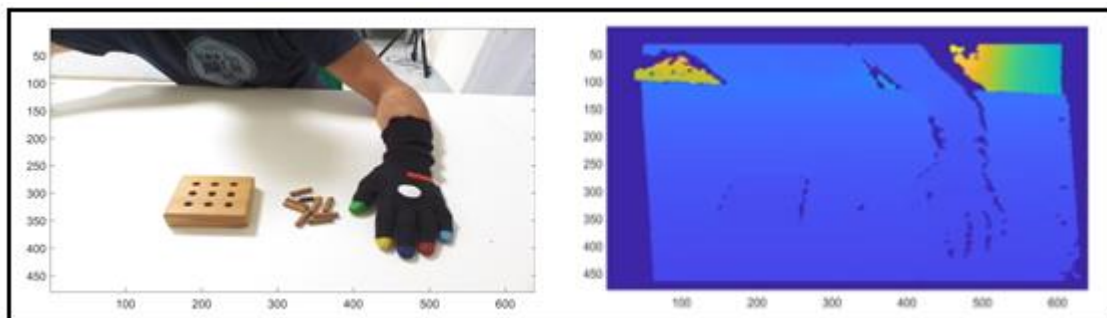


Figure 4.1: An example of RGB and depth images generated by the device

An example of depth image with the corresponding RGB image is shown in Figure 4.1. Warm colors of the pixels indicate points far from the camera, Cold colors indicate points near the camera, values set to 0 are associated to points for which the distance cannot be determined (to near or too far from the camera). Each camera has, in fact its own operative range for the estimation of the distance: for everything that is outside this range, the depth cannot be calculated reliably and therefore will be associated with the value 0. Operative range can vary from a few tens of centimeters (>30 cm) up to a few meters (3-5). In this context, the RGB-Depth image can be simply considered as the color image and the corresponding depth images combined.

In RGB-Depth cameras Depth and color image are produced by different sensors in the same physical device, therefore each of them has its own resolution. The resolution is generally specified during the initialization phase of the acquisition system according to the application needs. The resolution

determines the acquisition rate: in general the acquisition rate is lower if the resolution is higher when, for example, a higher quality of the final image is needed. The best compromise must be found between the image quality (resolution) and the acquisition rate (speed): this depends on the goals of the application. To guarantee the maximum acquisition rate to capture hand movements accurately for the activity described in this Master Thesis, the resolution has been set 640x480 both for color and depth images in order to acquire movement at 30 frames per second and to have a 1:1 match between points.

One of the main strengths of some cameras is that proprietary tracking algorithms (made available through the Software Development Kit or SDK) or algorithms developed by third parties are available for example to track human body movements. However, for almost all devices, it is possible to create dedicated tracking algorithms using Computer Vision and Machine Learning approaches since they provide the basic information needed. Apart from this, these devices are characterized by other strengths but also by weaknesses to be considered in the development of specific applications

Advantages of RGB-Depth cameras:

- ✓ Low cost
- ✓ Non-invasiveness: they allow contactless measurements
- ✓ Usability: they do not require complex calibration procedures
- ✓ Portability: they require only USB connection
- ✓ Versatility: they can be used for different applications

Possible problems related to the use of RGB-Depth cameras:

- ❖ occlusions: movements / objects may be hidden or not visible
- ❖ operative requirements: minimum and maximum operative distance, field of view, ambient light
- ❖ setup: need to choose the optimal settings for the context

4.3 Hardware of the acquisition system

The acquisition system is made up of the following elements: a RGB-D camera (kinetic v.1) a pair gloves with color markers, an elaboration unit (that could be a PC, a mini-PC or a notebook) with monitor. We want to point out that even if the Kinect v.1 is now out of production, it can be replaced in the setup by other models, without significant impact on the experimental results here obtained. Because of the availability of software already developed for the Kinect v1 firmware, the experiments were made by processing RGB and depth video streams at lower frame rates and resolutions with respect to those available with newer RGB-Depth cameras. The planned porting of the software to newer devices is expected to improve the system performance.

The acquisition system consists of Microsoft Kinect v.1 camera which provides synchronized RGB color and DEPTH streams at 30 frames/sec with resolution of 640 x 480 pixels (Figure 4.2). In RGB image, each pixel is associated to a triple (corresponding to the intensity of R,G,B channels) which together determine the color of a point. The RGB depth camera generates two types of “synchronized” information: color images where each pixel represents a color (in its three color components red, green and blue) and depth maps, that are a special images where each pixel represents the distance of a point of the observed scene from the device. The combination of the two information through appropriate re-projection algorithms, allows to switch from a two-dimensional point in the image to a three-dimensional point in the scene and therefore to achieve a metric reconstruction in real space.



Figure 4.2: The RGB-Depth Microsoft Kinect v.1 camera is equipped with RGB sensor, an IR depth sensor and an IR projector. From [40]

The user wears black silk gloves with imprinted color markers, which are used for tasks analysis and assessments.

The gloves are used to trace the movement of the hands and fingers through the identification of the colored blobs and their centroid through techniques and methodologies of Artificial Vision. Their function is to simplify the complex problem of developing a hand tracking algorithm that could be useful in the analysis of motor tasks as NHPT. A glove is shown in Figure 4.3. This solution has been successfully employed in the analysis of hand motor tasks related to Parkinson’s disease [41].



Figure 4.3: The colored gloves

The term Hand Tracking refers to the capture of the complex movements of the hand or part of it. This glove with colored markers has been used to develop a hand tracking algorithm based on the recognition and tracking of the color areas. It is a dedicated real-time algorithm, mainly based on Computer Vision techniques which integrate RGB and Depth information to ensure greater robustness to tracking and accurate kinematic measurements in 3D space. The tracking of colored markers is equivalent to track specific points of the hand, thus creating a hand tracking algorithm capable of capturing specific movements.

In the activity of this thesis, the colored glove is used to develop a new tracking algorithm dedicated to the NHPT test, which works in post-processing on the sequences of RGB and DEPTH images captured by the acquisition system to track the movement of the hand. In the near future, the hand tracking algorithm will be able to work in real-time.

As previously indicated, the first step is to define a setting to ensure the optimal capture of the movement of interest. So, a setup has been defined for the acquisition of the NHPT test, as shown in Figure 4.4.

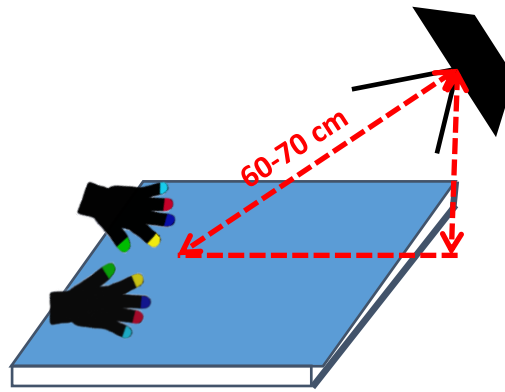


Figure 4.4: HAND-position and system set-up

The subject wears colored gloves keeping both hands on the support surface (one at a time depending on the limb to be examined). A working area has been defined on the table in which to perform the NHPT: in this way the working area will be the same for all the subjects examined and guarantees the maximum "comfort" compatible with the position required by the exercise.

The camera is positioned in front of the subject, with a view of the working area, and an inclination that allows the optimal framing of the hands during exercise. The distance on the diagonal must satisfy the operative constraints of the device considering that below a minimum distance (<50 cm), the adequate quality of the depth map (DEPTH) or the three-dimensional reconstruction of the movement would not be guaranteed. In addition, to ensure maximum stability and maximum control of the setup, the camera is mounted on a tripod so that it can possibly be raised, lowered and oriented easily. The setup does not require any specific calibration procedure.

4.4 Software of the acquisition system

The acquisition system is equipped with a dedicated software, running on the operator's PC, that allows for the acquisition of several motor tasks including the tasks of the MESUPES scale and the NHPT. Once the program is activated and after a series of initial checks on the correct connection of the RGB-Depth device, the following user interface is presented to the operator (Figure 4.5).



Figure 4.5: Activation of the program

The program allows the acquisition of three types of tests for analysis of upper limb motor function in post-stroke: "MESUPES", "NINE HOLES" and "FORZA". For each test the corresponding button has to be pressed to activate the acquisition. The "FINE SESSION" button will close the entire test session of the subject and has to be pressed by the operator only at the end of all tests planned for the subject. The green messages inform the operator of the progression of the system operation.

The program also includes the input of a simple patient card (Figure 4.6), where the operator can annotate the main information about the patient and the test session: this is useful for the statistical analysis on the collected data.

Figure 4.6: patient card

The field " Codice Identificativo Paziente " will allow the creation of the output directory to collect the data of all the tasks performed, while the field named " Lato Compromesso " will activate the correct scheduling of the various tasks (first with healthy limb, then with compromised limb). The field "Note Aggiuntive" allows the operator to enter some other significant information for the session in progress but it is not mandatory to enter notes, All the other field may be useful for statistical purposes.

Once the NINE-HOLES button has been pressed, the system will propose the acquisition for the healthy limb and then for the compromised limb: when the patient is ready, the operator activates the acquisition by pressing the "f" key which will last for a pre-set time maximum of 50 seconds. Before 50 seconds expired, the operator can decide to stop the exercise if the subject completes the positioning of the 9 pegs correctly or if an excessive fatigue is observed in the subject.

Once the healthy limb exercise is complete, the compromised limb exercise begins with the same mode.

The exercise with the healthy limb is indicated by the acquisition protocol to verify that the examined subject has correctly understood the exercise.

At the end of each exercise, the operator has to save the acquired information (RGB and DEPTH images) for the subsequent analysis phase.

The collected data are stored on the PC in a folder that contains the unique patient's code information, the date and start time of the session. Several sub-folders related to each exercise performed, are automatically created (Figure 4.7). The folders related to the hemiparetic side are indicated with the suffix "emi" to be easily identified. The data structure of a complete session is shown in the following figure:

Nome	Ultima modifica	Tipo	Dimensione
9HOLES_DX	31/01/2020 10:31	Cartella di file	
9HOLES_SX_emi	31/01/2020 10:32	Cartella di file	
FORZA_DX	31/01/2020 10:33	Cartella di file	
FORZA_SX_emi	31/01/2020 10:33	Cartella di file	
MESUPES_1_DX	31/01/2020 10:27	Cartella di file	
MESUPES_1_SX_emi	31/01/2020 10:29	Cartella di file	
MESUPES_2_DX	31/01/2020 10:28	Cartella di file	
MESUPES_2_SX_emi	31/01/2020 10:29	Cartella di file	
MESUPES_3_DX	31/01/2020 10:30	Cartella di file	
MESUPES_3_SX_emi	31/01/2020 10:30	Cartella di file	
MESUPES_4_DX	31/01/2020 10:28	Cartella di file	
MESUPES_4_SX_emi	31/01/2020 10:30	Cartella di file	
MESUPES_5_DX	31/01/2020 10:28	Cartella di file	
MESUPES_5_SX_emi	31/01/2020 10:30	Cartella di file	
MESUPES_6_DX	31/01/2020 10:20	Cartella di file	
MESUPES_6_SX_emi	31/01/2020 10:30	Cartella di file	
MESUPES_7_DX	31/01/2020 10:29	Cartella di file	
MESUPES_7_SX_emi	31/01/2020 10:31	Cartella di file	
MESUPES_8_DX	31/01/2020 10:29	Cartella di file	
MESUPES_8_SX_emi	31/01/2020 10:31	Cartella di file	
MESUPES_9_DX	31/01/2020 10:29	Cartella di file	
MESUPES_9_SX_emi	31/01/2020 10:31	Cartella di file	
ConfigDropbox.txt	21/05/2014 09:10	Documento di testo	1 KB
form.txt	31/01/2020 10:27	Documento di testo	1 KB
report_9holes_file.txt	31/01/2020 10:31	Documento di testo	1 KB
report_forza_file.txt	31/01/2020 10:33	Documento di testo	1 KB
report_mesupes_file.txt	31/01/2020 10:31	Documento di testo	3 KB
system_configuration.txt	31/01/2020 10:27	Documento di testo	1 KB
trace.txt	31/01/2020 10:27	Documento di testo	1 KB

Figure 4.7: The data structure

CHAPTER 5: Computer vision approach for the analysis of the 9 Hole Peg Test

5.1 Introduction

The purpose of this thesis work is to characterize the 9 Hole test automatically and objectively through kinematic parameters that can support the clinical evaluation of this test.

In general, the clinical evaluation of NHPT reports only the number of pegs correctly positioned in a certain time. The objective of this analysis is to verify if the evaluation through time and kinematic parameters could provide more information on the overall motor performance during NHPT. In this way, we can verify the improvement of rehabilitation treatments more effectively by means of objective measures.

This activity is based on the video sequences collected by the acquisition system described in the previous chapter and all the analysis was done through Computer Vision and Image Processing techniques by using the MATLAB environment and its programming language (The MathWorks R2019b).

The analysis procedure to reach an automatic evaluation of the test, required to solve the following topics:

- ✓ Automatic detection and tracking of hand
- ✓ Automatic detection and tracking of board
- ✓ Analysis of colour spaces representation on tracking robustness
- ✓ Holes detection on board
- ✓ Management of overlapping hand bounding boxes

5.2 Automatic detection and tracking of hand

The term tracking algorithm in general refers to an algorithm able of detecting an object, tracking it during its movement and estimating its trajectory. In this section, a hand tracking algorithm, developed by using the MATLAB tools and functions, is described.

This was the first step of the “procedure analysis”: the aim was to automatically identify the area where the hand was present (starting position) by applying an approach based on Color Segmentation. In particular, a segmentation mask for a color image (for example the first frame of the video sequence as shown in figure 5.1) was created by using Color Threshold App in MATLAB.

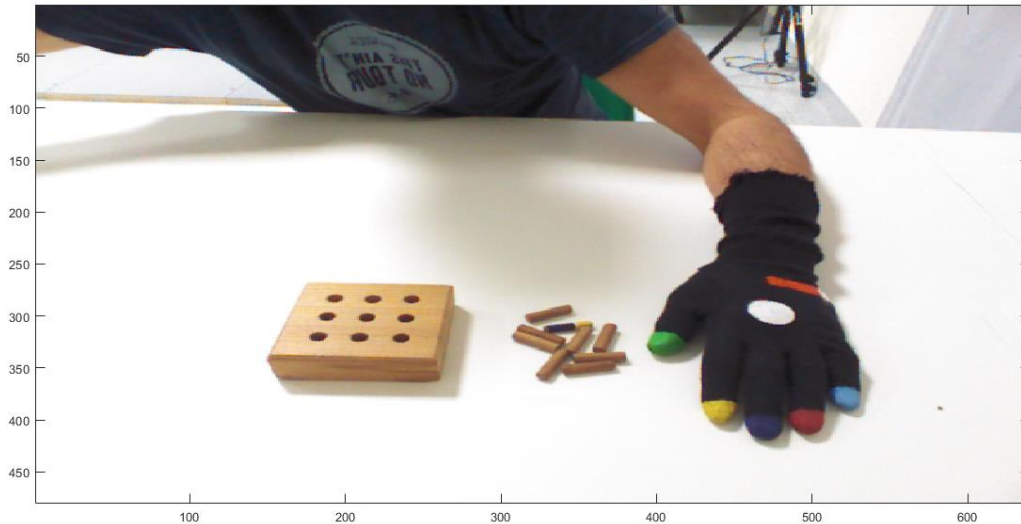


Figure 5.1: Original frame (RGB format) of the video sequence (starting position of the hand)

The Color Thresholder App allows to threshold color images by manipulating the color components of these images, based on different color spaces. This App is part of the Image Processing section of the MATLAB Apps menu. The first frame was loaded into the app as shown in Figure 5.2

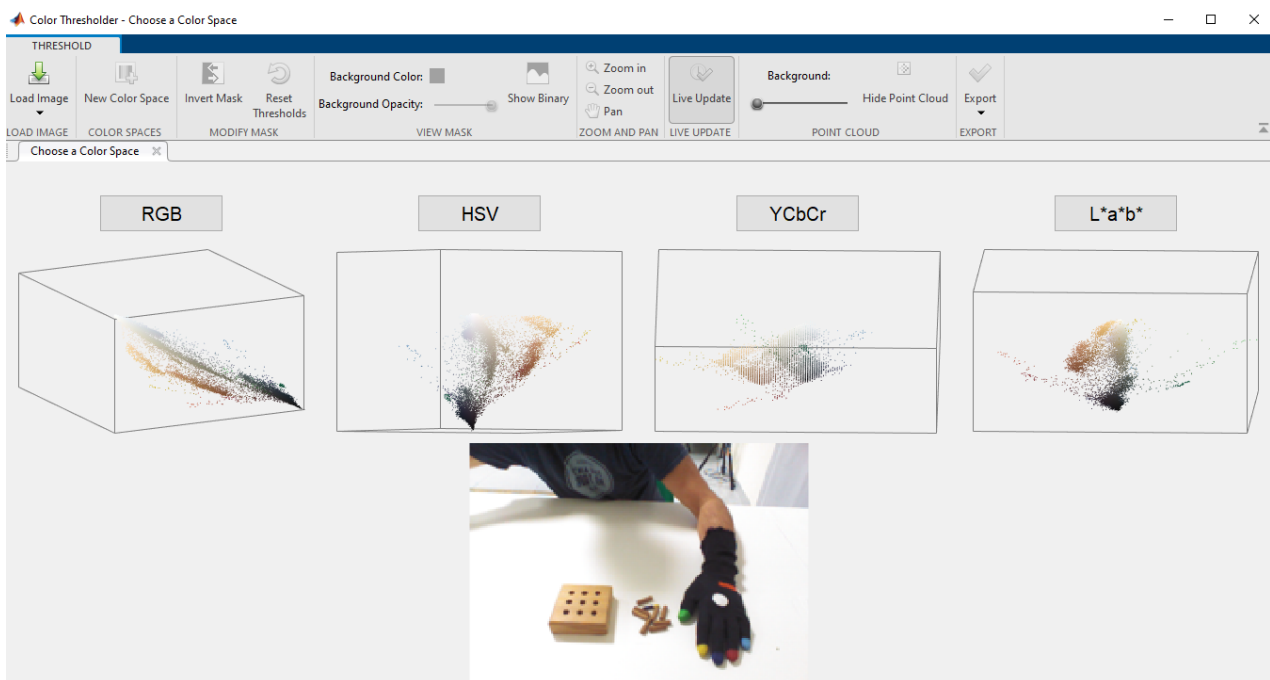


Figure 5.2: The Color Thresholder App

Initially, the RGB color space was selected and a region of interest was identified on the image preview as shown in Figure 5.3

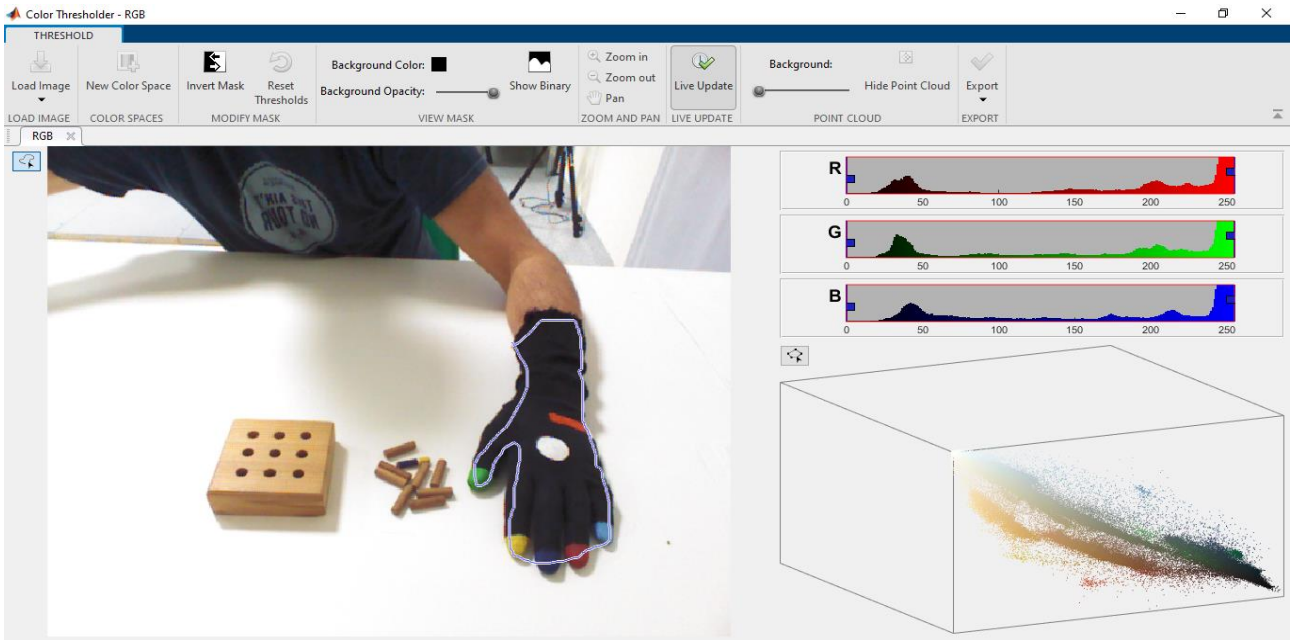


Figure 5.3: The Color Thresholder App was used to identify the hand

The color component sliders, shown on the top-right section of the App, were used to adjust the individual color thresholds for the mask as shown in Figure 5.4

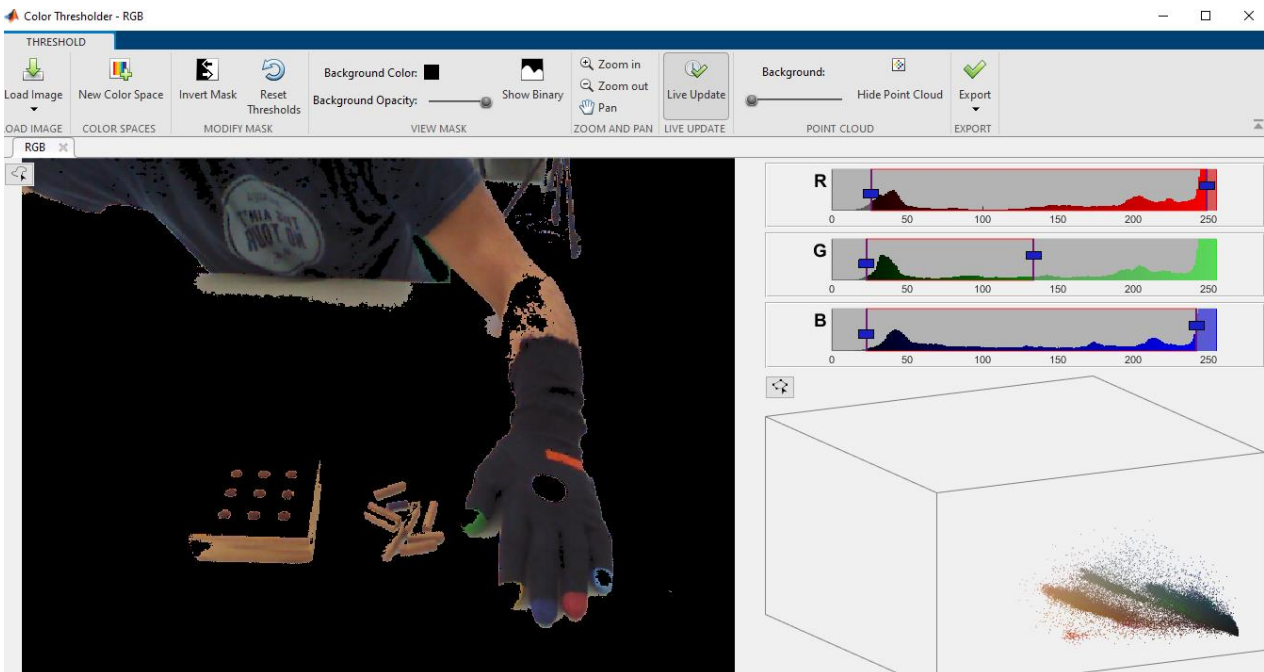


Figure 5.4: Color Thresholder automatically sets the image threshold based on the color of the hand

The threshold values for the three color components (R, G, B) have been identified to isolate the gloved hand by moving the three color sliders: in this way, only the color pixels of the image that fall within the range of the selected thresholds (minimum-maximum values) become part of the segmentation mask. An example of segmentation mask (Color Segmentation procedure) is shown in figure 5.5

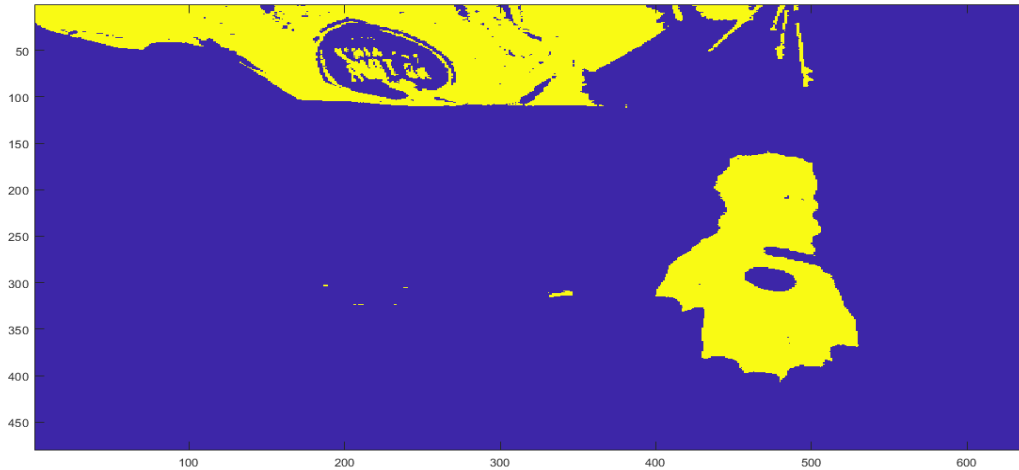


Figure 5.5: image mask obtained with color segmentation procedure

One of the problems that could occur using the Color Segmentation techniques is that color blobs, determined by setting the color thresholds, could be found everywhere in the scene observed by the optical device: this is evident in figure 5.5. In this case, the person performing the test wears a dark shirt which also satisfies the thresholds defined for the glove and this could generate confusion to the hand tracking algorithm. In fact, we assume that the color blob corresponding to the hand with glove is the biggest blob of the image: in this specific case, the area that corresponds to the shirt could result the biggest one and generates tracking errors. So, it is necessary to identify in the scene the region of interest (ROI) in which the hand with glove should perform the movement. To solve this problem, the depth image generated by the RGB-D optical device was used. As described in the previous chapter, the depth image is an image in which each depth pixel (which corresponds to an RGB pixel in the RGB image) represents the distance from the camera of the 3D physical point identified in the scene by the line of sight defined by the depth pixel and the center of optical system of the camera. According to the point of view of the optical device, the hand is closer to the camera (i.e., at lower distance) while the person is further away (i.e. at higher distance). This information can be used to isolate by the depth information the region of interest (ROI) and to work only on it, namely the area in which the hand moves during the test.

In the depth image the pixel area of having a distance less than 700 mm was selected: this approximately corresponds to the volume in front of the user, where there is the table area on which the board is placed and the movement is performed. The distance Segmentation mask and the bounding box of this area (bb_mask) was determined (Figure 5.6 right) and used for all the frames (in fact, this area doesn't change during the task).

The Distance Segmentation Mask is used to define the foreground area reduce the area of the RGB image where the hand tracking algorithm works to track the hand movement, as shown in figure 5.7

right. Color blobs outside the foreground area are not considered, and assigned to the background areas (as for example the shirt in figure 5.5).

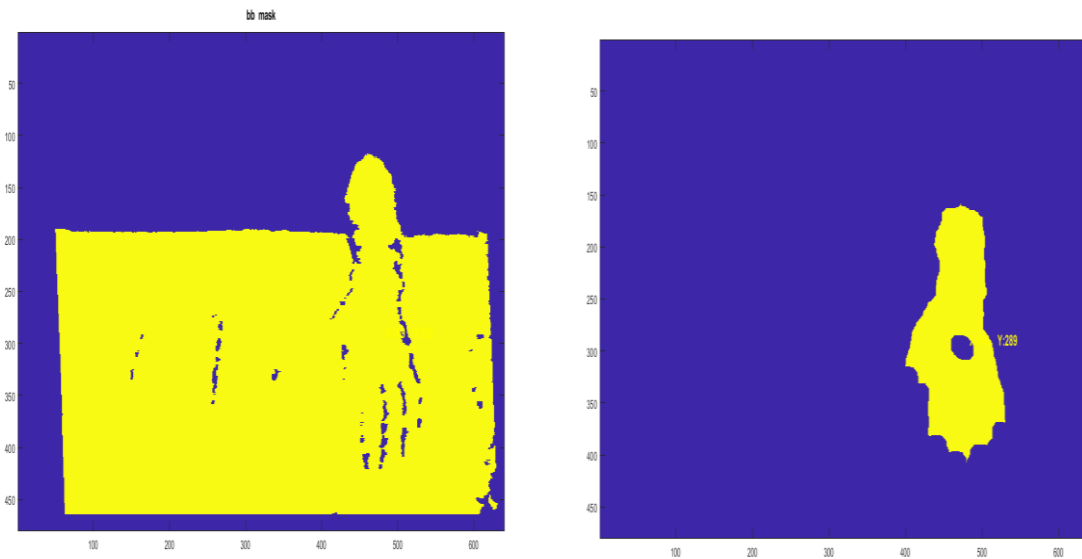


Figure 5.6: Left: Depth Segmentation mask obtained from the first frame; right: the result of color segmentation procedure after the application of Depth Segmentation mask on the first frame.

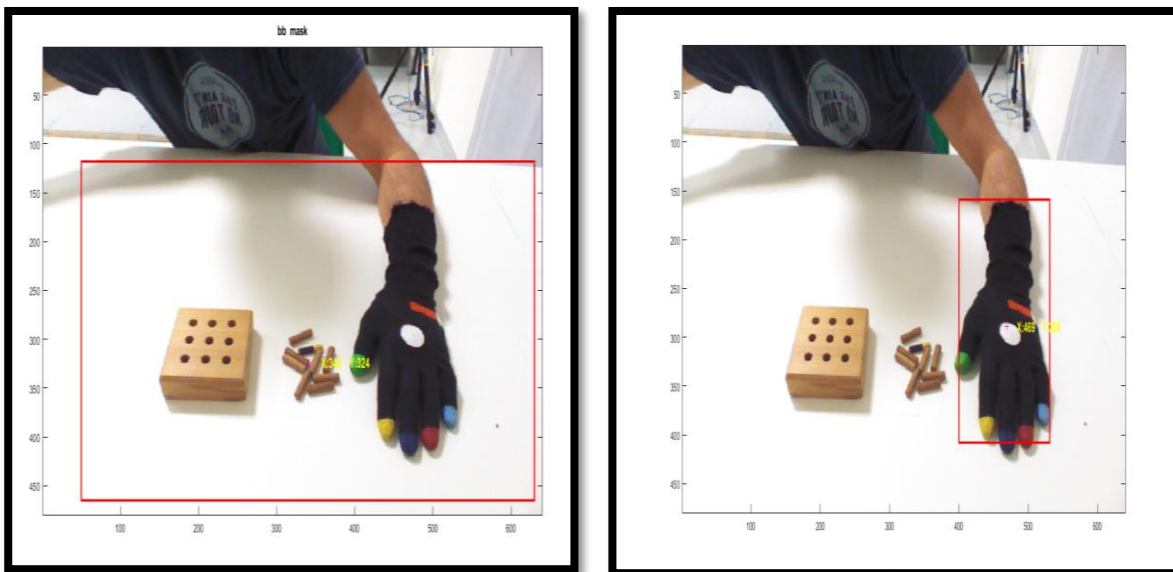


Figure 5.7: Left: RGB image with the bb mask on the first frame; right: RGB image showing the bounding box of the hand after the application of the Distance Segmentation mask on the first frame

After this procedure, the hand tracking algorithm can detect and track the hand without errors. The MATLAB function **regionprops** was used to compute the Bounding Box of the hand with glove (i.e., the area in the region of interest that satisfies the color thresholds defined) and to calculate the centroids for connected components in the frame, as shown in figure 5.8.

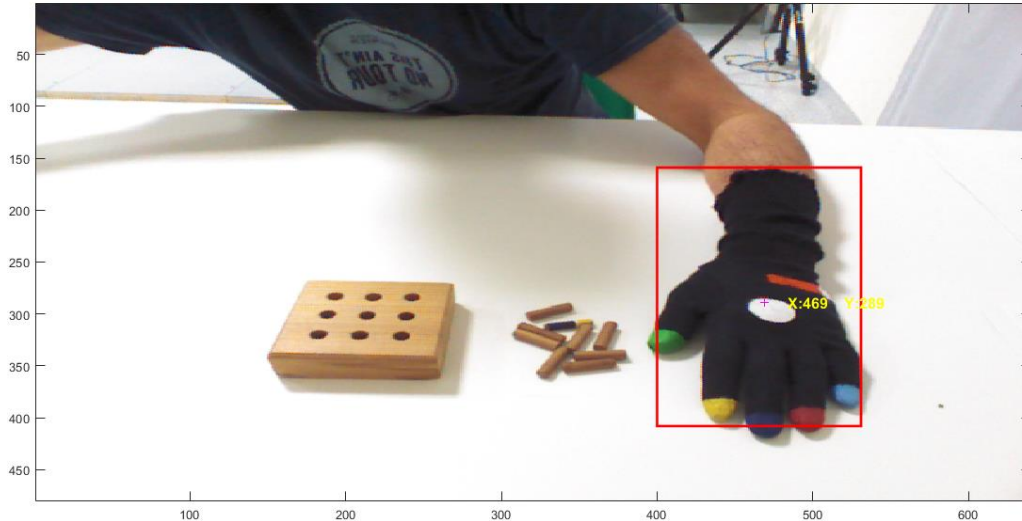


Figure 5.8: Detection of the hand in the first frame. Both the Bounding box and its centroids (2D position on the image) are shown.

The same procedure was applied to all the frames of the video sequence. Differently of the first frame, in which the starting position of the hand ensures high visibility and makes detection and tracking easier, the visibility of the hand could not be optimal during the movement, causing problems to the hand tracking algorithm.

For example, one of the problems was the detection of two bounding boxes of the hand instead of single one, as shown in figure 5.9. This happens in some frames of the analysed video sequence, as if two distinct objects, had satisfied the color thresholds, generated by unconnected color blobs.

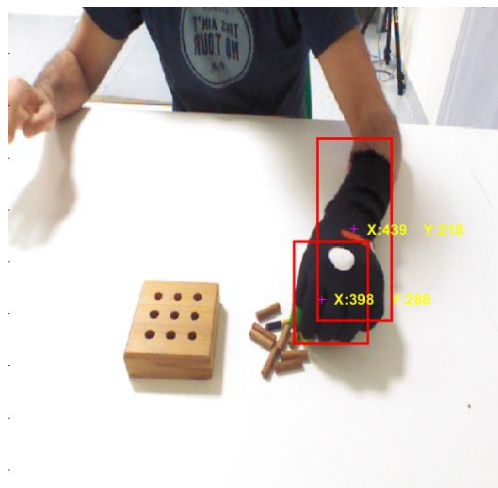


Figure 5.9: Detection of two bounding boxes on the hand

To solve this problem, two solutions were examined :

- 1) Applying the **bwareafilt** function: **bwareafilt**(BW,n) extracts the n largest objects from the binary image representation BW (n=1 was used to extract only the largest blob). This function returns a binary image (BW2) containing only those objects that meet the criteria. This MATLAB function can be used to extract only the largest blob, as shown in Figure 5.10, but this solution causes jumps of the centroid position on the basis of which bounding box is considered.

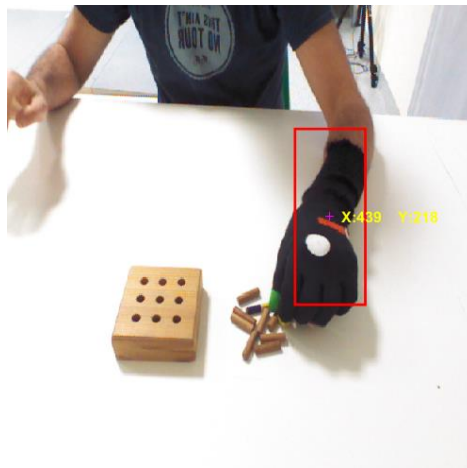


Figure 5.10: Example of bounding Box selection when the **bwareafilt** is used

- 2) Applying the **imclose** function, this MATLAB function can be used to join two blobs by creating a unique bounding box, as shown in Figure 5.11.



Figure 5.11: Example of bounding Box selection when the **imclose** is used.

After analysing all the frames of the video sequence, the solution based on **imclose** was preferred as it ensures greater stability over time of the centroid of the hand bounding box.

At the end of the procedure described in this section, two results were achieved:

- The automatic detection of the initial position of the hand. **This allowed to avoid the manual selection of the initial position with the mouse, moving towards an automatic analysis procedure:** the centroid of the hand bounding box in the initial frame was used instead of manual section (mouse coordinates).
- The tracking of the hand with glove during the test execution. The trajectory of the hand movement consists of the 2D centroid of the hand bounding box for each frame of the sequence

5.3 Automatic detection and tracking of board

In this section, the goal was to automatically identify the area in which the board was present by applying an approach based on Color Segmentation as for the hand. In particular, a segmentation mask for the board was created from a color image (for example, from the first frame of the video sequence as shown in figure 5.1) by using the Color threshold App in MATLAB on RGB color space. The result of Color Segmentations procedure is shown in Figure 5.12

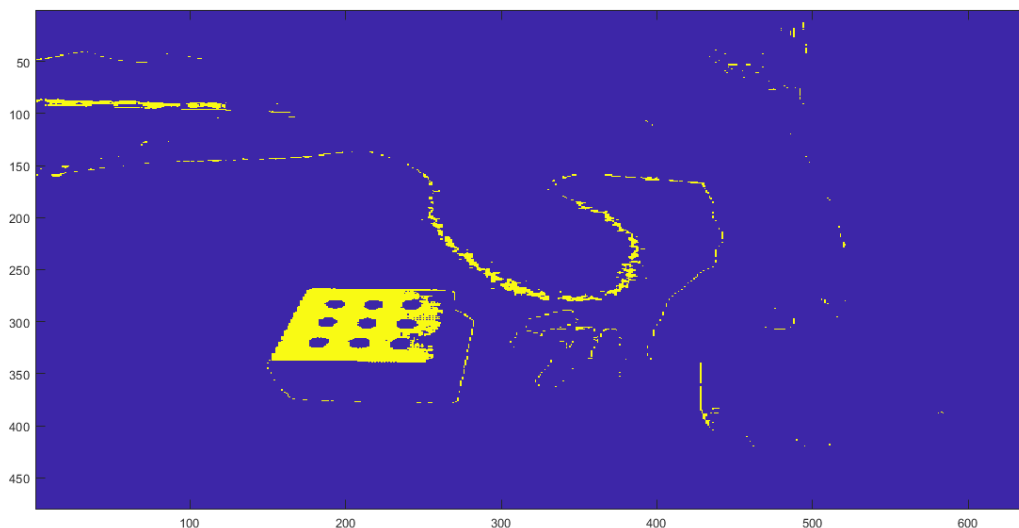


Figure 5.12: image mask obtained with color segmentation procedure

After this procedure, the board tracking algorithm can detect and track the board without errors. This procedure is required to avoid involuntary board movements caused by the user during the test performance. The MATLAB function **regionprops** was used to compute Bounding Box of the board (i.e., the area in the region of interest that satisfies the color thresholds defined) and to calculate the centroids for connected components in the frame, as shown in Figure 5.13

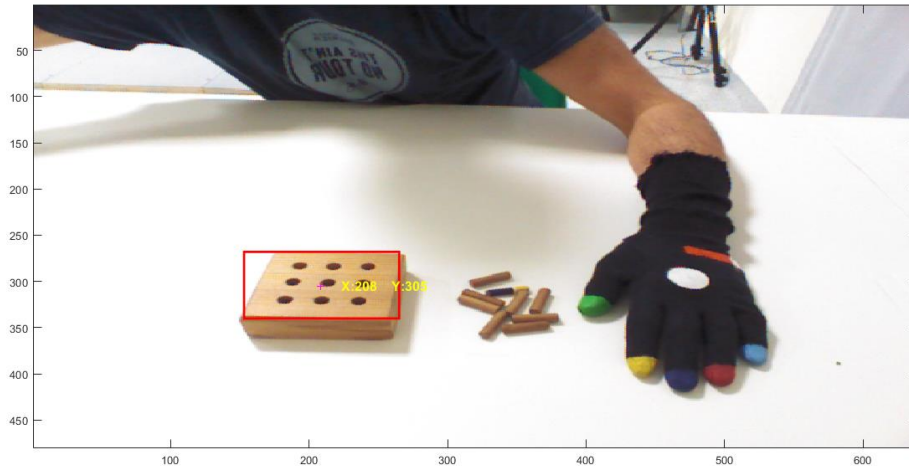


Figure 5.13: Board detection and tracking

5.4 Analysis of colour spaces on tracking robustness

A colour image can be classified as a set of multiple layers of grayscale images where each layer of the image corresponds to a certain band in the visible light spectrum [42]. The information that is stored in each layer of the colour image is the brightness in a specific spectral band. The most commonly used spectral bands are red(R), green (G) and blue (B), the three primary colours in the visible range of the electromagnetic spectrum, The RGB colour bands chosen correspond to the absorption characteristics of the human eye and give the RGB color space representation of the image. While the RGB space may be the best representation for many applications (e.g. television) it suffers from a number of serious limitations ad discussed in the rest of the section.

In the HSV colour space the scene luminance information is represented in the V layer and the chromaticity information in the H and S layers. The separation of the brightness information from the chrominance and chromaticity in the HSV colour spaces reduces the effect of uneven illumination in an image.

The use of the chrominance and chromaticity information of the HSV representations enables more robust tracking algorithms to be developed than those based on the grayscale and RGB colour spaces. The HS layers in the HSV colour space, contain sufficient information for more accurate tracking compared to grayscale and RGB images [42].

HSV is less sensitive to changes in ambient light. This could be useful to robustly analyse other sequences that have been obtained in different light conditions.

Depending on the used colour space, an effect on tracking performance could be present. For this reason, both the RGB and HSV colour spaces were examined for the analysis of the video sequences, to compare the performance of the tracking algorithm by using the two color spaces.

The Color Thresholder APP was used to define the threshold values for the three components (R, G, B) on the image in the RGB color space: the threshold values (integers between 0-255) that have been identified to isolate the gloved hand and the board, are shown in table 5.1.

	R(red)		G(green)		B(blue)	
	Minimum Threshold	Maximum Threshold	Minimum Threshold	Maximum Threshold	Minimum Threshold	Maximum Threshold
Hand	20.000	70.000	20.000	70.000	20.000	70.000
Board	213.000	255.000	165.000	255.000	63.000	194.000

Table 5.1: Thresholds set in the RGB color space

The Color Thresholder App was then applied to the image in the HSV color space. The App was used to determine the thresholds for the three components (H, S and V): these thresholds were obviously different from the ones for RGB spaces, because the components of the two color spaces contain different information. The threshold values for HSV color space are shown in table 5.2.

	H(hue)		S(saturation)		V(value)	
	Minimum Threshold	Maximum Threshold	Minimum Threshold	Maximum Threshold	Minimum Threshold	Maximum Threshold
Hand	0.006	0.001	0.000	0.341	0.000	0.212
Board	0.048	0.998	0.149	0.532	0.842	1.000

Table 5.2: Thresholds set in the HSV color space

The figure 5.14 shows the difference between two image masks obtained with the color segmentation procedure in the HSV and RGB color spaces to isolate the board

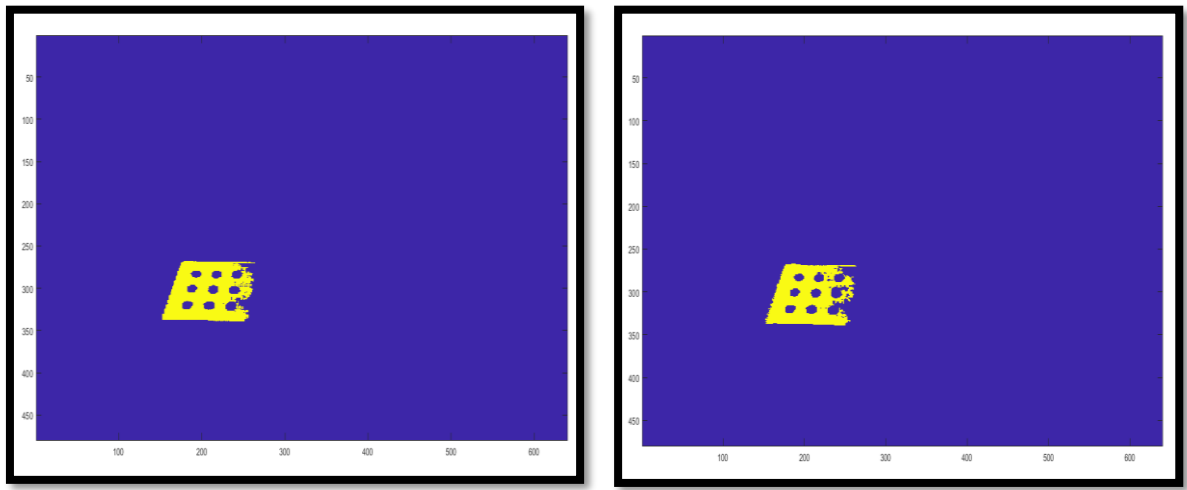


Figure 5.14: Depth image (left) showing image mask for the board applied on the first frame in RGB color space, Depth image (right) showing image mask applied on the first frame in HSV color space

The figure 5.15 shows the difference between the two masks obtained in the RGB color space and HSV color space to isolate the gloved hand. As can be seen in figures 5.16 and 5.17, the thresholds determined for the two color spaces, RGB and HSV respectively, allow to correctly isolate both the hand and the board.

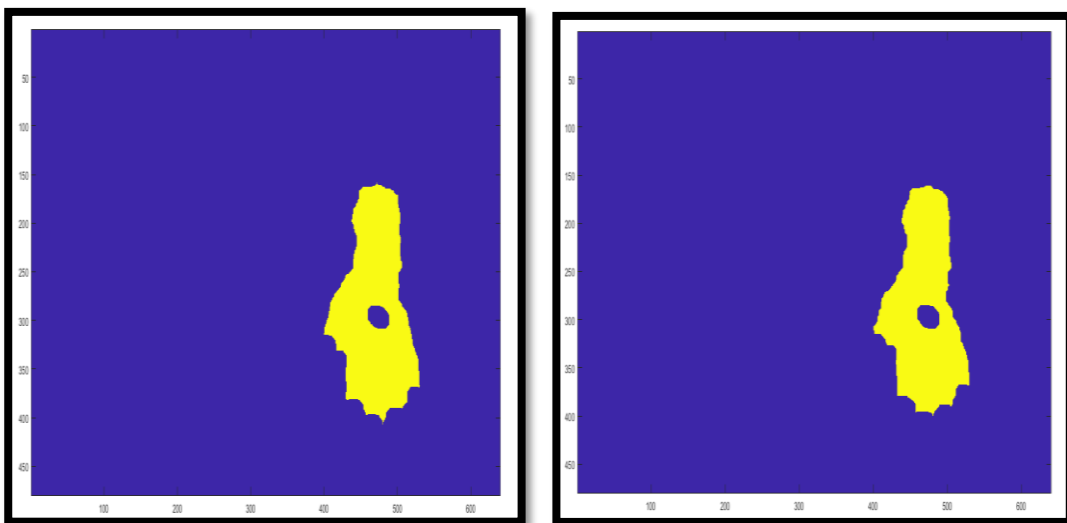


Figure 5.15: Depth image (left) showing image mask for the glove applied on the first frame in RGB color space, Depth image (right) showing image mask applied on the first frame in HSV color space

In this thesis work it was decided to work on RGB color space and HSV color space as shown in Figure 5.16 and figure 5.17.

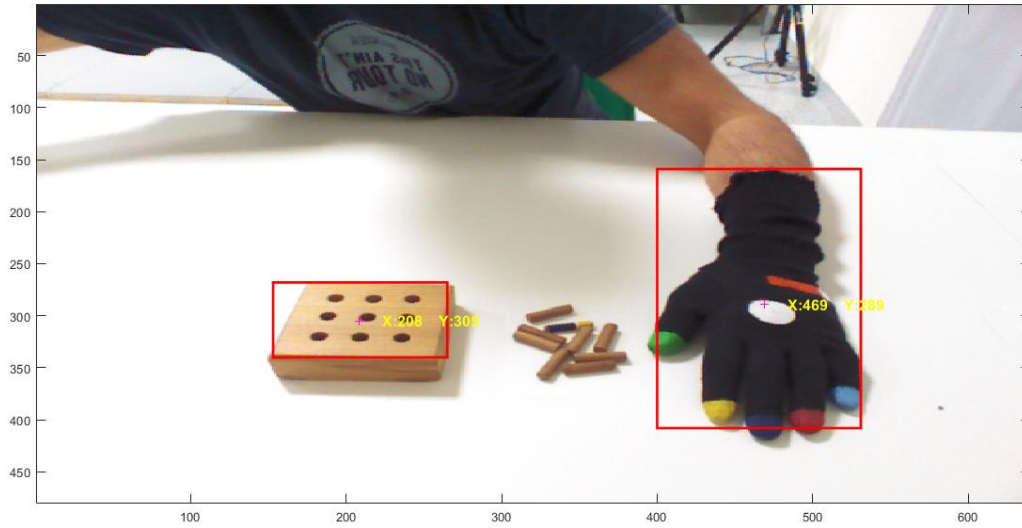


Figure 5.16: Automatic detection and tracking of hand and board for RGB color space (first frame of the video sequence)

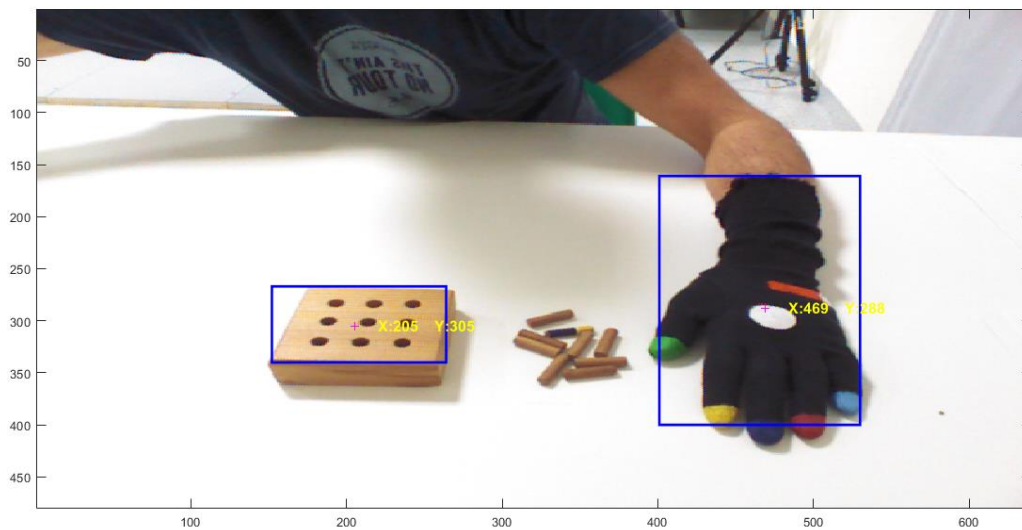


Figure 5.17: Automatic detection and tracking of hand and board for the HSV color space (first frame of the video sequence)

In the first frame, the centroids of the bounding boxes obtained in the two color spaces coincide: this is because in the first frame there is no movement, and everything is optimally visible. On the other hand, when the hand is moving, the centroids do not necessarily coincide because it depends on how the two objects (hand and board) are "seen" and segmented by the tracking algorithm

Figure 5.8 shows an example of the real position of the two centroids in RGB color space and in HSV color space on the hand in frame #381. Figures 5.18 and 5.19 are synchronized, and hence, they refer to the same instant in time.

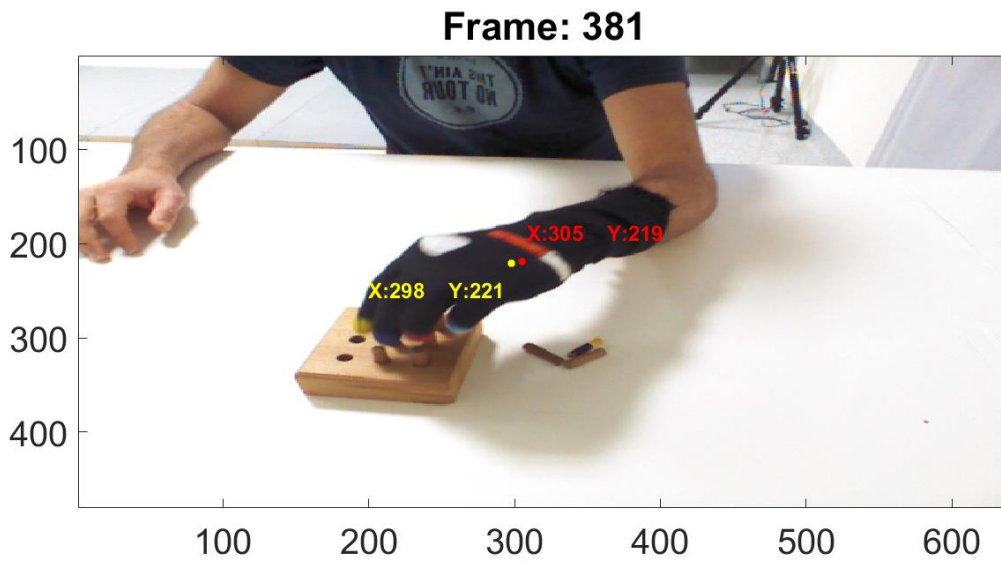


Figure 5.18: Two centroids of the hand in RGB color space (yellow) and in HSV color space on the hand (red) in frame #381

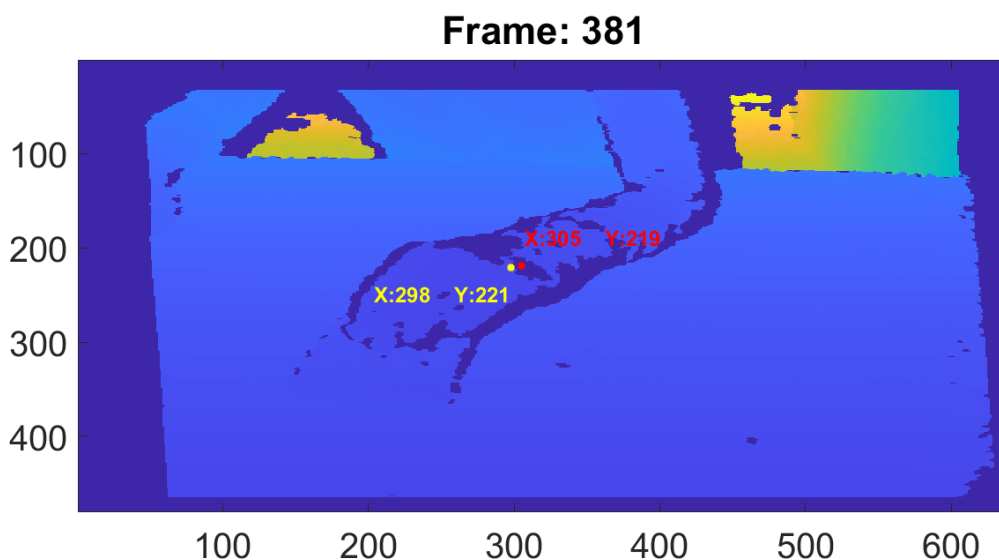


Figure 5.19: Depth image showing the two centroids of the hand in RGB color space (yellow) and in HSV color space on the hand (red) in frame #381

In this case, the position of the centroids related to the two color spaces is different.

The reason for the difference between the two centroids is due to how the gloved hand is "seen" during this dynamic phase (the hand is in movement and the motion blurring and the noise affect the final position of the centroid differently in the two color spaces), while in figures 5.20 and 5.21 , where the hand is in the initial position, the two hand centroids ,for RGB and HSV color spaces are almost superimposed

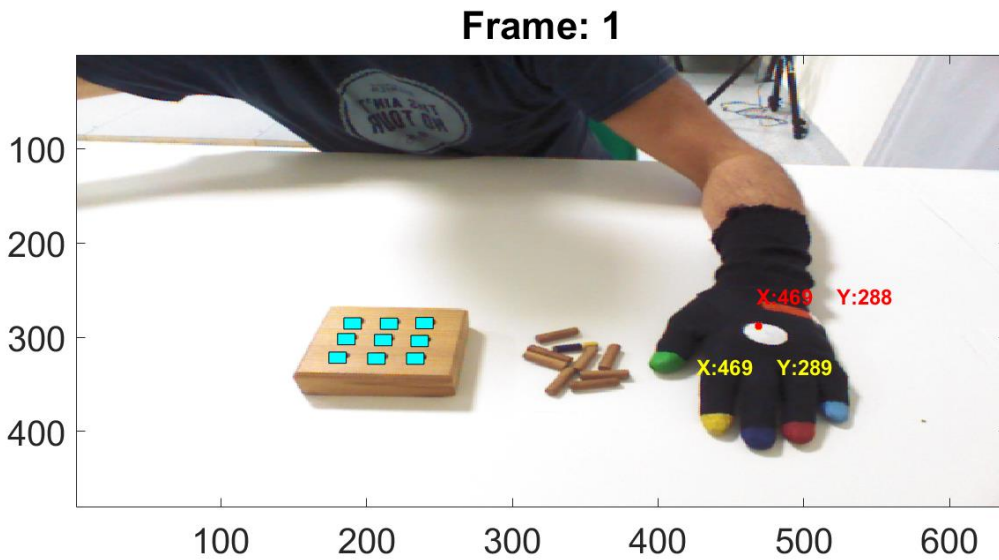


Figure 5.20: Color image showing, the two centroids of the hand in RGB color space (yellow color) and in HSV color space on the hand (red color) in frame #1

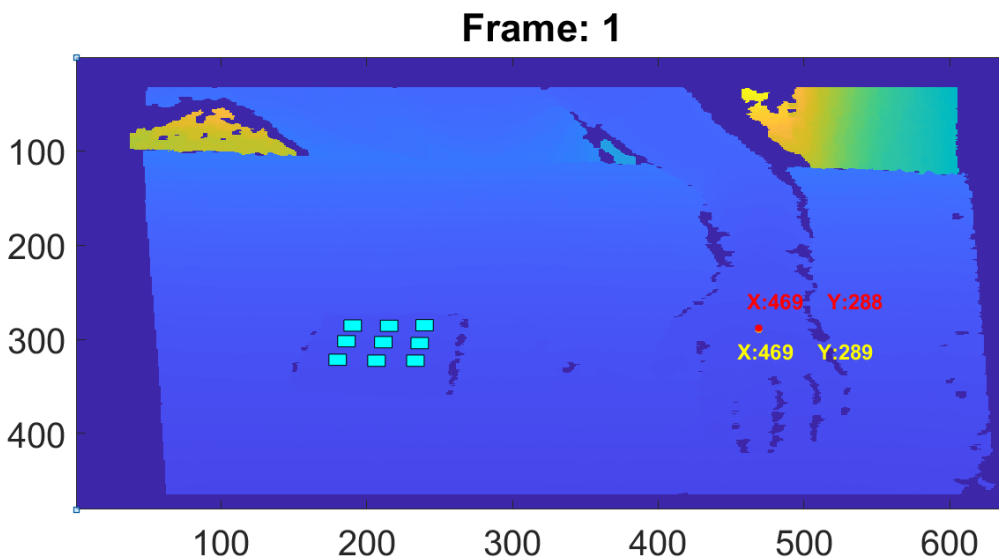


Figure 5.21: Depth image showing, the two centroids of the hand in RGB color space (yellow color) and in HSV color space on the hand (red color) in frame#1

The difference between the X coordinate of the centroid of the hand bounding box in the RGB color space (X_{rgb}) and the X coordinate of the centroid of hand bounding box in the HSV color space (X_{hsv})

has been calculated. The graph in figure 5.22 shows that the tracking algorithms in the two color spaces produce minimal differences on the X component.

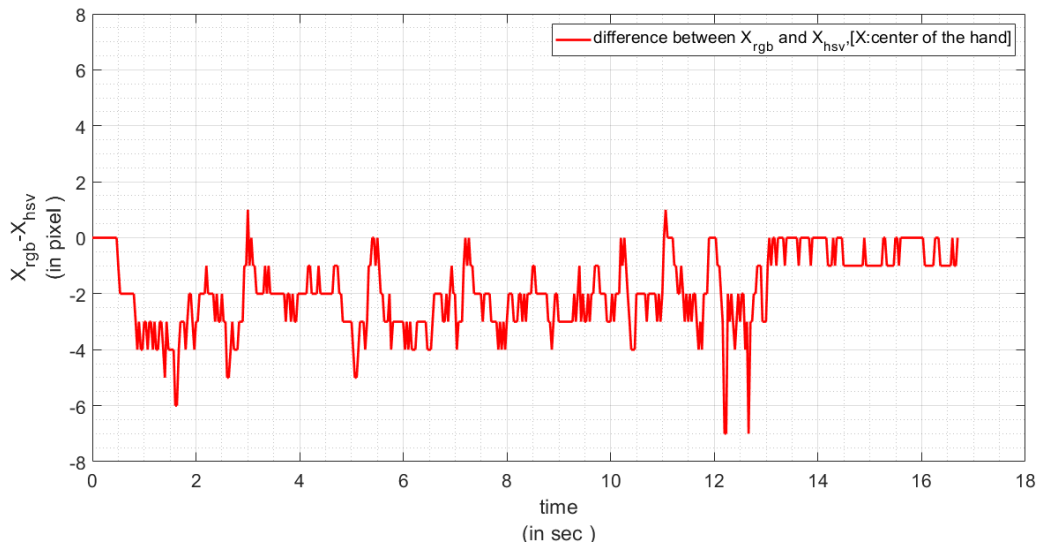


Figure 5.22: Difference between X_{rgb} and X_{hsv} versus time.

The difference between the Y coordinate of the centroid of the hand bounding box in the RGB color space (Y_{rgb}) and the Y coordinate of the centroid of hand bounding box in the HSV color space (Y_{hsv}) has been calculated.

The graph in figure 5.23 shows that the tracking algorithms in the two color spaces produce minimal differences on the Y component

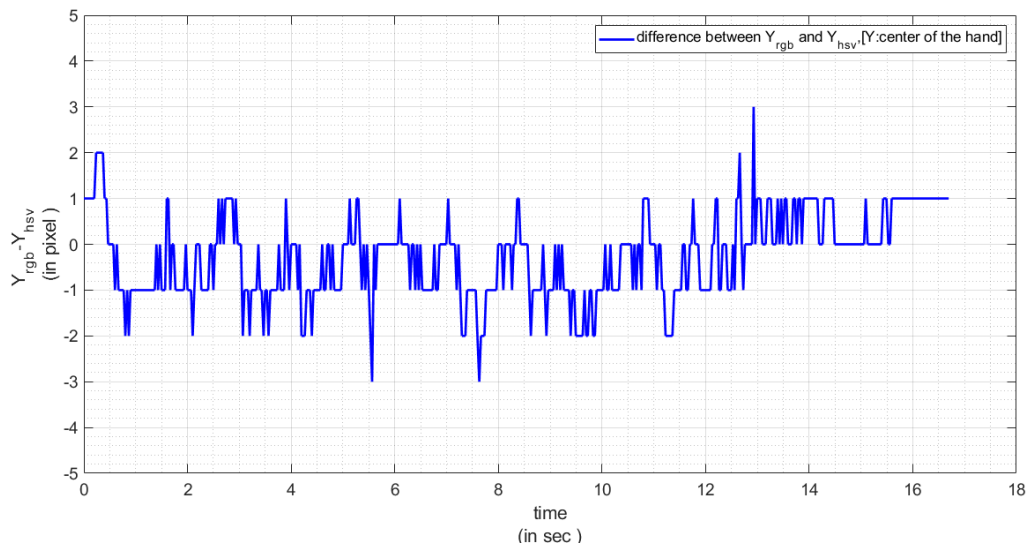


Figure 5.23: Difference (in pixel) between Y_{rgb} and Y_{hsv} versus the time.

The mean value of the difference between X_{rgb} and X_{hsv} and the mean value of the difference between Y_{rgb} and Y_{hsv} is shown in the following table

Parameter Name	Parameter Value
Mean value of the difference between X_{rgb} and X_{hsv} (in pixel)	-1.924
Mean value of the difference between Y_{rgb} and Y_{hsv} (in pixel)	-0.266

Table 5.3: Mean values of the difference between pixel coordinates of the centroids evaluated in RGB and HSV color spaces

5.5 Holes detection on the board

The clinical evaluation of the NHPT is based on the number of pegs placed into the holes of the board. The automatic analysis should determine the same information: the goal is to understand how many pegs are inserted into the board during the time assigned for the test completion. In this section, the procedure to determine the number of pegs is described.

Several approaches could be used to determine the number of pegs correctly inserted on the board. Considering that the board and the pegs have same color, it is difficult to identify the pegs using the colour thresholds estimated for the board. Then, another approach was considered based on the Holes Detection techniques, a group of algorithms that search for “holes” within an image. In particular, an approach that works only on color images (2D approach) to find the holes on the board and not the pegs, was used by applying typical techniques of image processing. The number of pegs (N_{PEGS}) placed at a certain time can be determined as the difference between the starting number of holes on the board (i.e.,9) and the current number of holes (N_{HOLES}) detected.

$$N_{PEGS} = 9 - N_{HOLES}$$

Starting from 9 initial holes on the board, the algorithm should detect fewer holes each time a peg is correctly inserted. The number of holes should therefore drop (from 9 to 0) during the test.

The area of the image relating to the board has been transformed into a grayscale image as shown in the figure 5.24

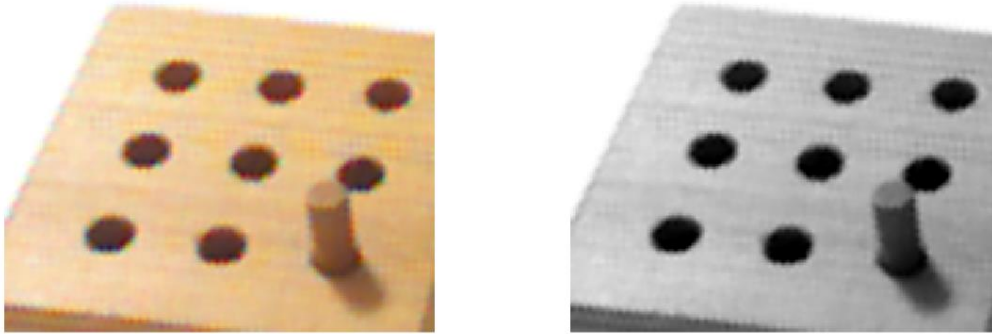


Figure 5.24 : Left: original image, right: figure shows grayscale image

The brightest parts (corresponding to the board) and the darkest parts (corresponding to the holes) are detected by a threshold. Then, some morphological filters have been applied to clean up the mask obtained in order to remove isolated points (small areas) and to better highlight the holes. The results is shown in figure 5.25



Figure 5.25: Left: board before applying the morphological filters, right: board after applying the morphological filters.

Since the holes are quite small, after applying the morphological filters any areas that are too large compared to the possible size of the holes, also will be eliminated. The morphological filters also serve to give shape to the remaining blobs in order to facilitate the detection of the circles.

The MATLAB function **imfindcircles** was used to determine the location of all circles with a radius between 10 to 20 pixels: this range was set according to the size of the board holes. Based on the outlines returned from **imfindcircles**, the function **viscircles** was used to display full circles as shown in Figure 5.26.

The MATLAB function **imfindcircles** was applied only when the board is totally free: this means when bounding boxes of hand and board are not overlapped, not even partially. The parameter **bright** was used to find all the bright circles in the image within the radius range.

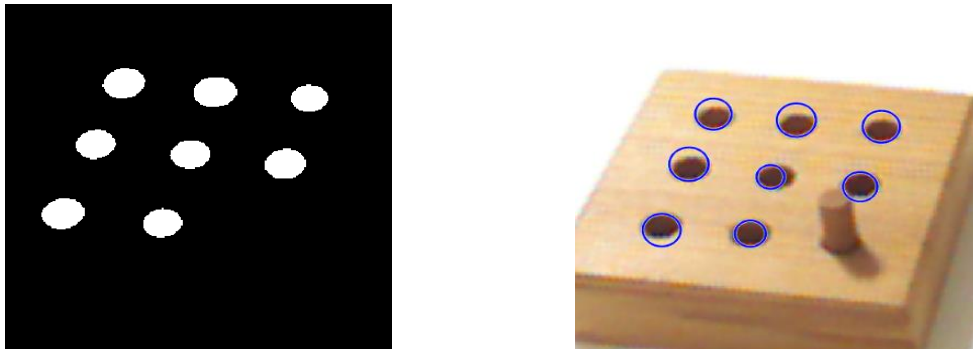


Figure 5.26: The circular holes detected by the **imfindcircles**. The circles are displayed using the **viscircles** function.

Imfindcircles is an unstable function, especially in detecting small circles: for this reason, the morphological filters were applied on the hole mask to increase the size of the holes. This function allows to specify some parameters as input, which, depending on the case, can work better or worse. It may happen that some circles are not detected or that some false positive are returned. This is a problem that may cause a wrong number of holes detected, both during the execution of the test and at the end of the same. As shown in figure 5.27 multiple circles are detected for the same hole, causing a wrong number of holes detected on the board as shown in figure 5.28

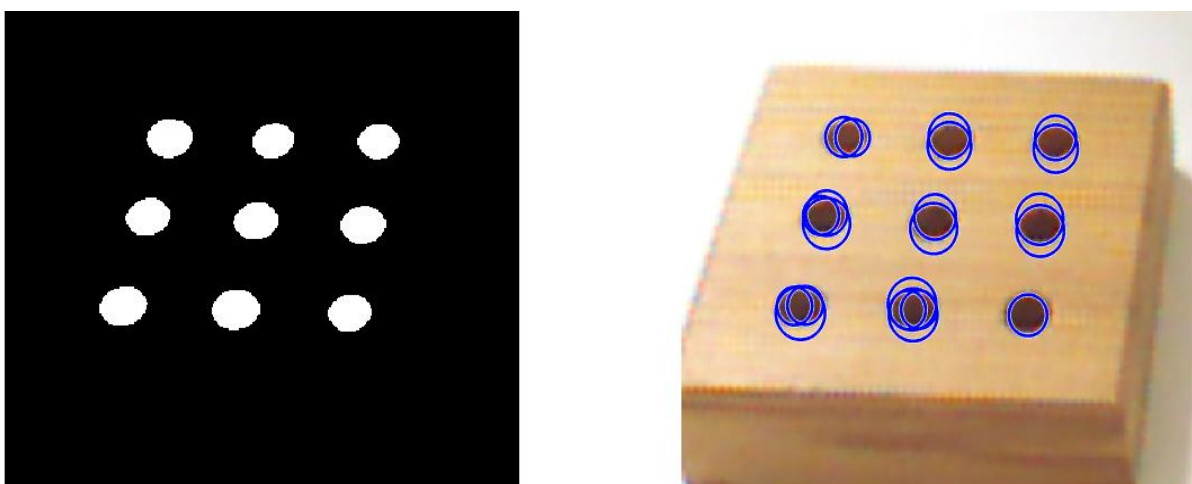


Figure 5.27: Example of multiple circles detected for the same hole.

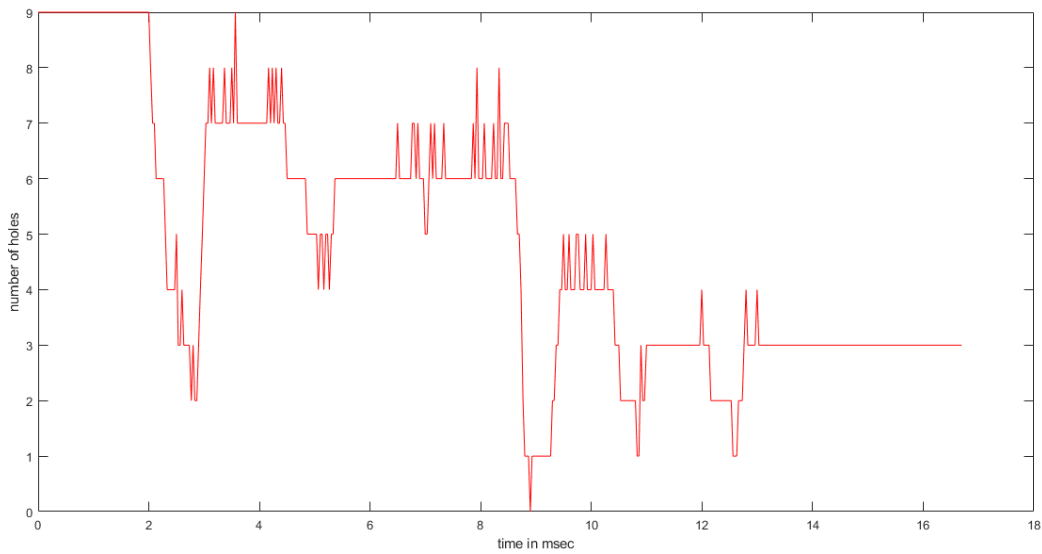


Figure 5.28 : Y axis: the number of holes detected on the board; X axis: the time spent from the starting of the test

To solve this problem an algorithm was added to the holes detection procedure. This algorithm checks all the found circles to eliminate duplicates, based on the radius and the distance between each other. Two circles can be considered the same circle when the distance between their centers is less than the sum of their radius: in this case, only one circle is maintained while the other is discarded.

The pseudo-code of the algorithm is the following:

For i=1: to number of circles

For j=1: to number of circles

Calculate d_{ij} as Euclidean distance between the centers of i and j circles

Calculate k as the sum of the radius of i and j circles

If $d_{ij} < k$ && radii(j) > 0 then

centers(i,1)=null

centers(i,2)=null

radii(i)=null

end

end

At the end of this algorithm, the number of circles detected is equal to the number of visible holes, as shown in figure 5.29.

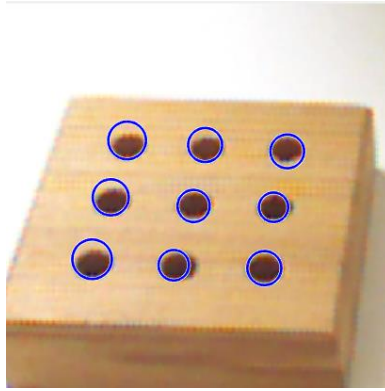


Figure 5.29: Correct number of holes after removing multiple circles

At this point, two results were achieved:

- ❖ The correct number of holes is detected on the board after solving the problems related to `imfindcircles` function, as shown in figure 5.29
- ❖ The number of holes detected correctly decreases during the test execution.

At the end of this procedure, the number of holes detected monotonically decreases (so the corresponding number of pegs monotonically increases) during the test execution.

An example showing the results for the case of six pegs inserted is shown in figure 5.30 and 5.31.

The graph of the holes detected is shown in figure 5.19.

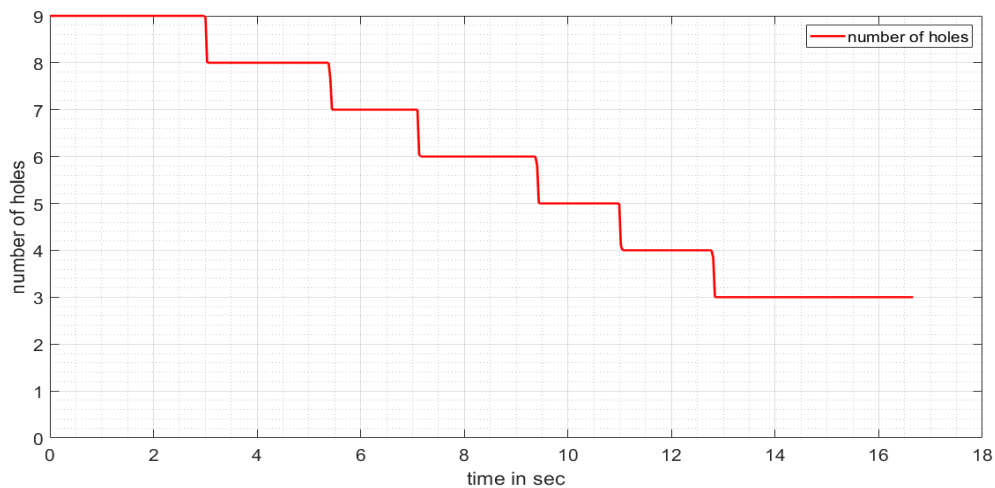


Figure 5.30: Correct number of holes detected on the board as function of time.

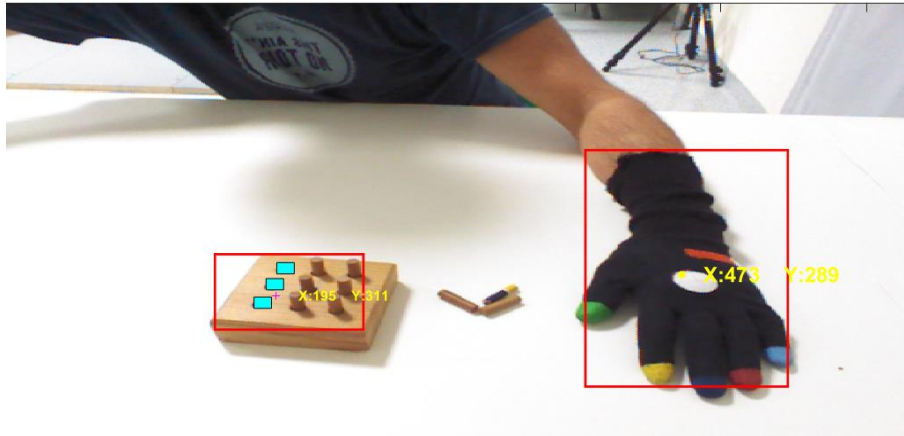


Figure 5.31: RGB image showing that the test was completed with 6 pegs inserted

In figure 5.31 is shown the final frame corresponding to the end of the test.

At this point, three basic elements for the analysis of the 9 Holes Peg Test were developed:

- ✓ The automatic detection and tracking algorithm of the hand,
- ✓ The automatic detection and tracking algorithm of the board,
- ✓ Robust and accurate detection algorithm for the holes on the board.

The three algorithms work on all frames of the video sequence simultaneously: the result for the first and the last frame is shown in Figure 5.32

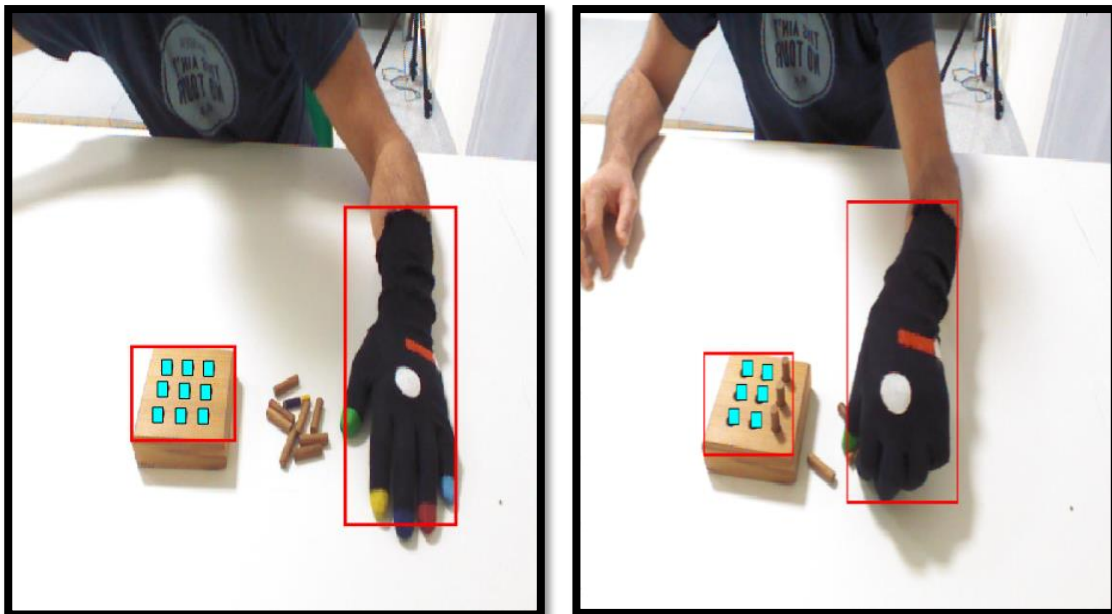


Figure 5.32: Board tracking, hand tracking and holes detection (first frame of the video sequence)

5.6 The management of overlapping bounding boxes

During the execution of the test, there are periods in which the hand, is exactly above the board, for example during pegs positioning. This causes occlusion and the impossibility to correctly estimate the holes on board. In fact, when the hand is partially on the board, the algorithm is not be able to

detect the holes correctly because part of the board and some holes are not visible, causing an incorrect number of holes detected (Figure 5.33).

To solve this problem, a different strategy was adopted: the algorithm for detecting holes is applied only when the board is totally free of occlusions: this means when bounding boxes of hand and board are not overlapped, not even partially.

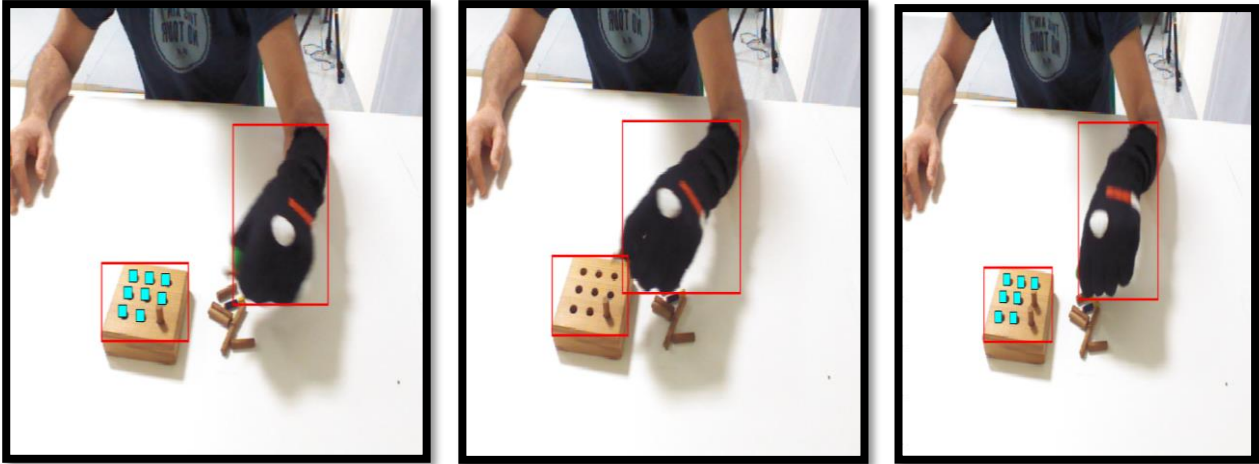


Figure 5.33: Left holes detection algorithm is applied; on the center: holes detection algorithm is suspended (bounding boxes partially overlap); Right: holes detection algorithm is resumed.

To determine when an overlapping between bounding boxes is present, the MATLAB function **bboxOverlapRatio** was used. This function returns the **overlapRatio**, a value between 0 and 1, where 1 implies a perfect overlapping between two bounding boxes.

When the **overlapRatio** is less than 1 the two bounding boxes are partially overlapped; when the **overlapRatio** is equal to 0 the two bounding boxes are not overlapped as shown in figure 5.34. This condition was checked before applying the holes detection algorithm to determine the current number of holes. On the contrary, when an overlap is detected as shown in figure 5.35, the algorithm is suspended, and the number of holes is maintained equal to the last estimation.

At the end of this procedure, the following result was achieved:

-for each frame of the sequence, it was determined if the holes detection algorithm can be applied.

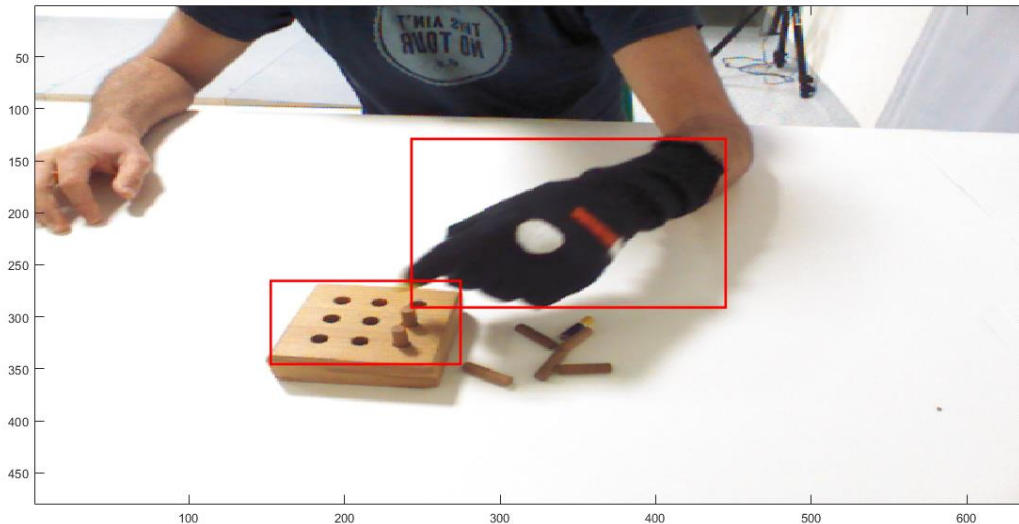


Figure 5.34: Example of overlapping between the two bounding boxes: the `overlapRatio` is less than 1 (`overlapRatio= 0.0193`) denoting a partial overlapping

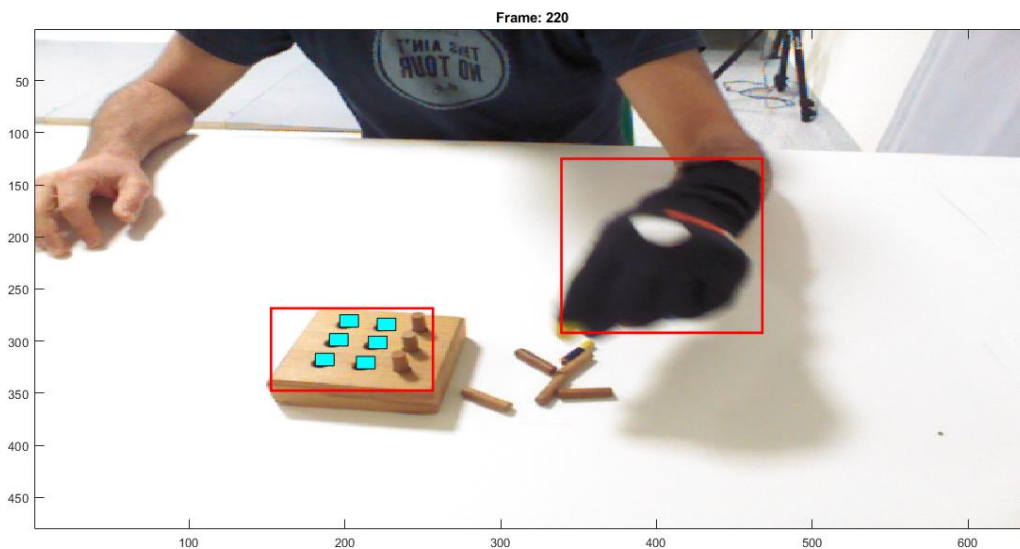


Figure 5.35: Example of no-overlapping condition between the two bounding boxes: in this case `overlapRatio` is zero.

5.7 Automatic detection of the start and endpoint of the test

To correctly analyse the NHP, it is important to establish when the test starts and ends, by checking the hand movement condition

The idea is that the test starts when the hand starts to move both in position (with respect to the initial hand position) and in height (with respect to the initial hand depth). For the position, the hand movement (movement condition) was detected when the pixel percentage of the hand in the initial bounding box obtained on the first frame is less than a threshold (that, for these experimental tests

was set to 35%). On the contrary, when the percentage is greater than the threshold, the hand is considered in steady condition.

For the height, the difference between the depth of the center of the hand bounding box in the initial position and in the following frames was considered to determine the hand movement. When the difference (as absolute value) is greater than 10 cm, the hand is considered in movement condition, otherwise the hand is in steady condition.

The instant in which both the “movement” conditions are satisfied is considered as the starting point of the exercise. On the contrary, when the hand returns to the initial position at the end of the exercise, the “steady” conditions are checked: the instant in which both the “steady” conditions are satisfied is considered as the ending points of the exercise.

The period between the automatically detected starting and ending points of the exercise is used for the movement analysis of the exercise.

5.7.1 The trajectory of the hand in 2D space

In this section, the goal was to graph the trajectory of the hand during the movement. In particular, the 2D Euclidean Distance between the center of the hand bounding box during the movement and the initial hand position (i.e., the center of the hand bounding box in the first frame) was considered and calculated.

The Euclidean Distance between $P1(x_1, y_1)$ and $P2(x_2, y_2)$ was calculated in the following way:

$$\text{Euclidean Distance} = \sqrt{((x_1 - x_2)^2 + (y_1 - y_2)^2)}$$

In this context, the analysis of the movement trajectory is important, as it can provide significant information from a clinical point of view on how the exercise was performed, allowing to highlight, also through its graphic representation, the presence of any anomalies.

As previously mentioned, two-colour spaces, (RGB and HSV) were used to analyse the video sequences: for both, the hand trajectories were calculated. An example of hand trajectories is shown in figure 5.36. It is clear that there is not much difference between the two estimated trajectories; this result implies that the hand tracking algorithm seems to work correctly in both cases. These trajectories need to be verified with further experiments by comparison with gold-standard reference systems for motion analysis (i.e. optoelectronic systems).

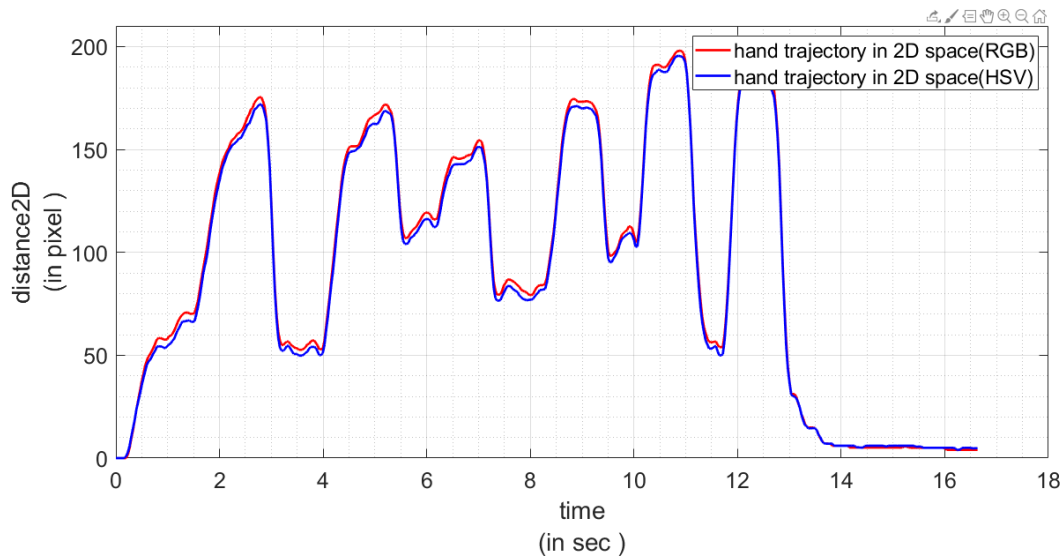


Figure 5.36: 2D distance (in pixel) between initial and actual bounding box position of the hand vs time (in seconds) for RGB color space (red) and HSV color space (blue) representation.

The difference between the trajectories obtained in the two color spaces is negligible, as expressed by the Root Mean Square Error (RMSE), which is calculated according to the following formula (MATLAB):

$$\text{RMSE} = \sqrt{\text{mean}(\text{P1} - \text{P2})^2}$$

Where P1, P2 are two-time corresponding points taken respectively from the trajectories HSV and RGB described in figure 5.36

This is shown in figure 5.37.

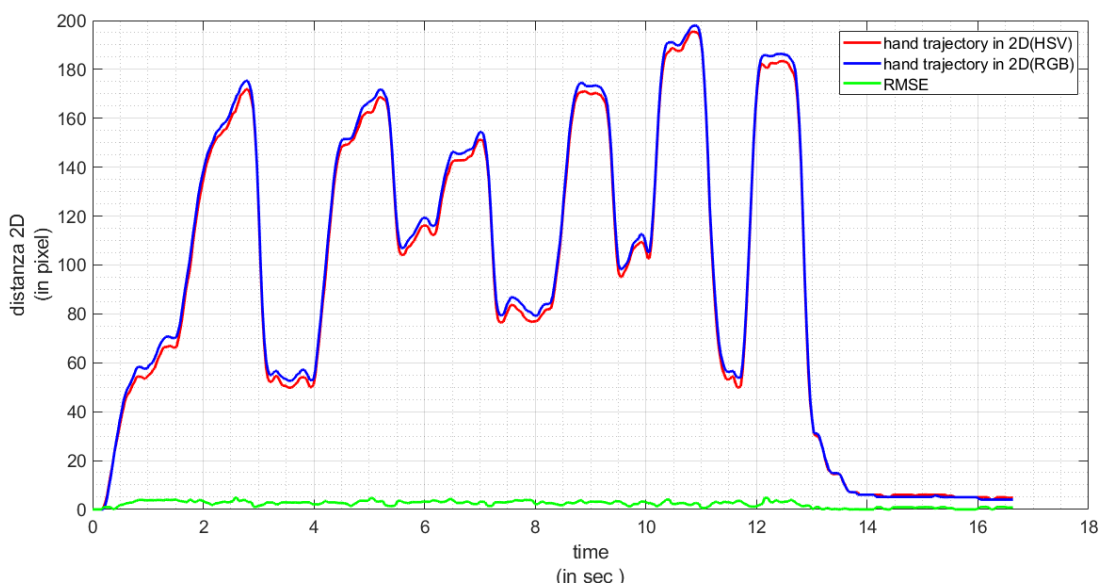


Figure 5.37: The same graphs of Fig.5.35 with the RMS error between the two trajectories (green line)

The Mean Standard Deviation, Maximum and Minimum values of RMSE over all the points of the trajectories are shown in the table 5.3: these values confirm that the tracking algorithms in the two color spaces have similar performance and are both robust and accurate in tracking the hand movements.

In this work we have not explored the effect of large lighting variation on the tracker performance, typical of real home environment, because of the limited time available for the experiments and the lack of true ground as reference. However, we note from the results on color space representations that the HSV color space is less sensitive to light variations, it can therefore be considered a valid alternative to RGB in the case of uncontrolled lighting conditions.

2D trajectory differences parameters	Value (in pixel)
mean	2.24
standard deviation	1.3
Min_RMSE	0
Max_RMSE	6.430

Table 5.4: Mean and standard Deviation , Max and Min values of RMSE (in 2D space)

5.7.2 The trajectory of the hand in 3D space

The hand trajectory can be transformed from 2D space (pixel coordinates) into 3D space (coordinates in real space) by using the information provided by the depth map information associated to the color image. In this way, it is possible to obtain information and estimate kinematic measurements of movement in real space.

In practice, the 2D pixels of the color image can be transformed into their corresponding 3D position in real spatial coordinates (X, Y, Z). For this conversion, two pieces of information are needed: the 2D coordinates of a point (Px,Py) on the color image (for example, the centroid of the hand bounding box) and the corresponding distance measure (expressed in mm) obtained from the depth image provided by the RGB-Depth camera .

We make use of registered pairs of color and depth images provided by the camera firmware. that is the color and depth images are alignment. This means that the pixel (Px, Py) on the color image, represents the image of a 3D scene point whose distance value from the camera stored in the (Px, Py) pixel on the depth image

It is possible that the distance estimation algorithm is not able to determine a "depth" value for all the pixels in the image, assigning them an "undetermined" value corresponding to "0": a "0" value of depth prevents the transformation from 2D to 3D space .To overcome this problem it was decided to consider the "neighbour" of the "0" value pixels made of the 3x3 matrix adjacent pixels. In this case

the distance associated with the reference pixel will be the average of the distances of the neighbour pixels involved in the 3x3 matrix (excluding the ones with “0” values).

To estimate the 3D trajectory of hand movements, each 2D centroid of hand bounding box (P_x, P_y) was converted to 3D coordinates with respect to the reference system of the camera. Then the 3D Euclidean Distance between $[X_p, Y_p, Z_p]$ and the initial 3D position of the hand estimated for the first frame $[X_0, Y_0, Z_0]$ was calculated.

The Euclidean Distance between $P_1 (x_1, y_1, z_1)$ and $P_2 (x_2, y_2, z_2)$ was calculated as indicated in the following formula:

$$\text{Euclidean Distance} = \sqrt{((x_1 - x_2)^2 + (y_1 - y_2)^2 + (z_1 - z_2)^2)}$$

The 3D trajectories in RGB color space and HSV color space were calculated as shown and figure 5.38 shows the results. Also, in this case, the goal is to verify that the two trajectories are similar and characterized by low differences in 3D real space.

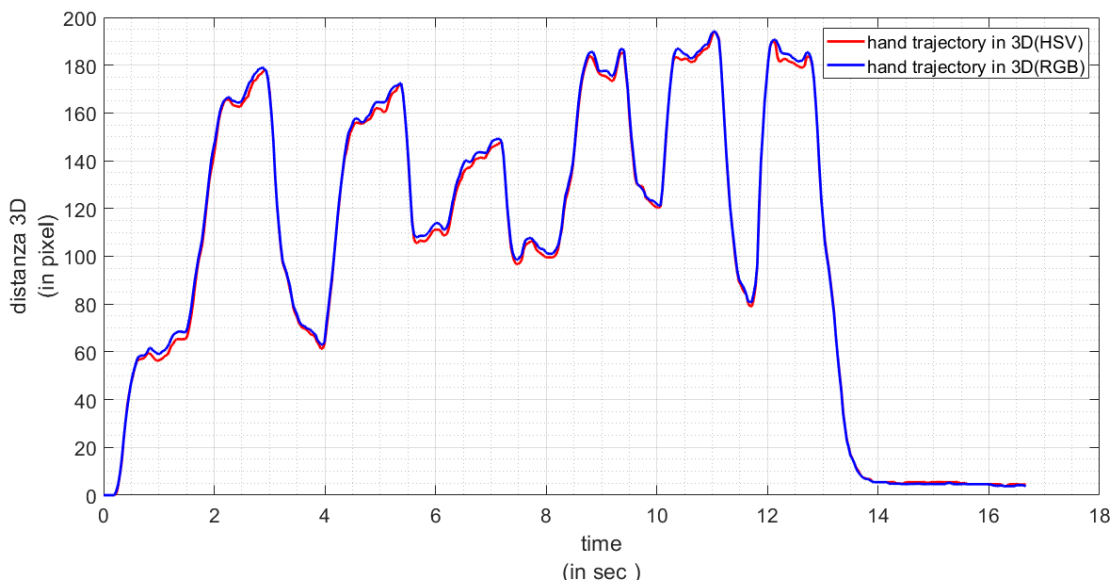


Figure 5.38: The distance between the trajectories of the hand in 3D space vs time, both in the HSV color space (red color) and in RGB color space (blue color) respectively

Again, the Root Mean Square Error (RMSE) was calculated as described in the previous paragraph and the graph of RMSE was added in figure 5.39.

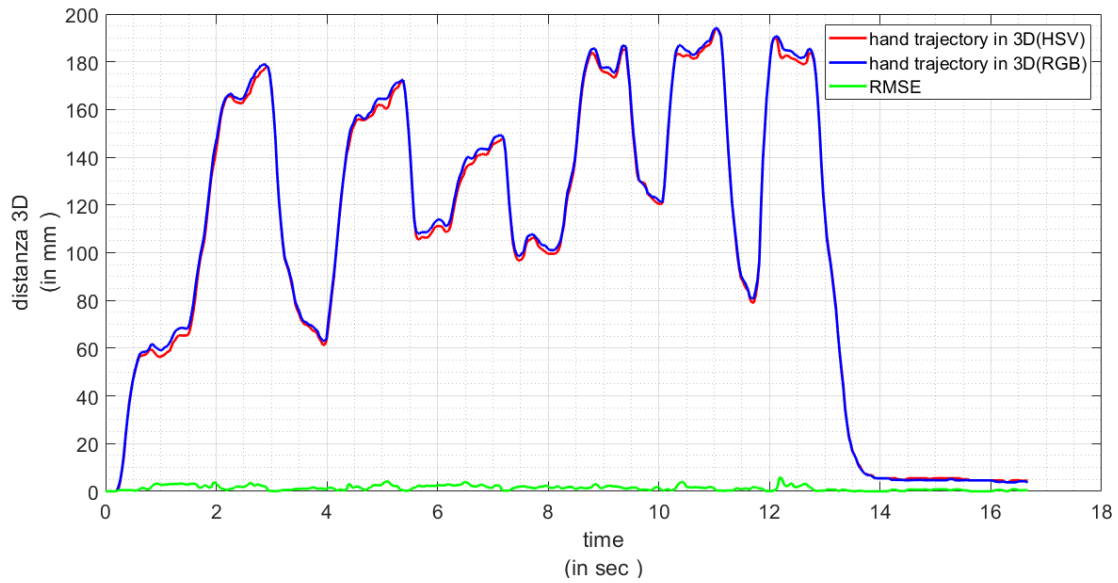


Figure 5.39: The same graphs of Fig. 5.37 with the RMS error between the two trajectories (green line)

The mean value and standard deviation are shown in table 5.5

3D Trajectory differences parameters	Value (in pixel)
Mean	1.3811
Standard Deviation	1.1323
Min RMSE	0
Max RMSE	8.093

Table 5.5: Mean and standard deviation, Max and Min values of RMSE (in 3D space)

From the graph of figure 5.39 the following parameter has been extracted (as described in section 5.10):

- ✓ Quantity of Hand Movements

5.8 The graph " hand in Movement"

According to the procedure described in Section 5.7, the following algorithm was added to the analysis procedure to check if the hand is moving or not.

The pseudo-code of the algorithm is the following:

```
For i=1:to "number of frames"  
    If the percentage of hand in the initial area >threshold  
  
        Save the "current depth" corresponding to the initial hand position.  
  
        if abs ("current depth" - "initial depth") <10 cm then  
            in movement(i) = 0; % hand steady  
        else  
            in movement(i) = 1; % hand in movement  
        end  
    else  
        in movement(i) = 1; % hand in movement  
  
    end  
end
```

At the end of this algorithm, the graph "hand in movement" is generated, as shown in figure 5.40.

The total duration of the exercise was calculated based on the "in movement" vector: the first transition 0-> 1 in the vector "in movement" determines the instant of the beginning of the test; the last transition 1-> 0 of the vector "in movement" determines the end of the test. The difference between the times associated to the events is considered as the duration of the exercise. If other transitions were detected, these could be significant from a clinical point of view, denoting a form of uncertainty in starting or ending the exercise.

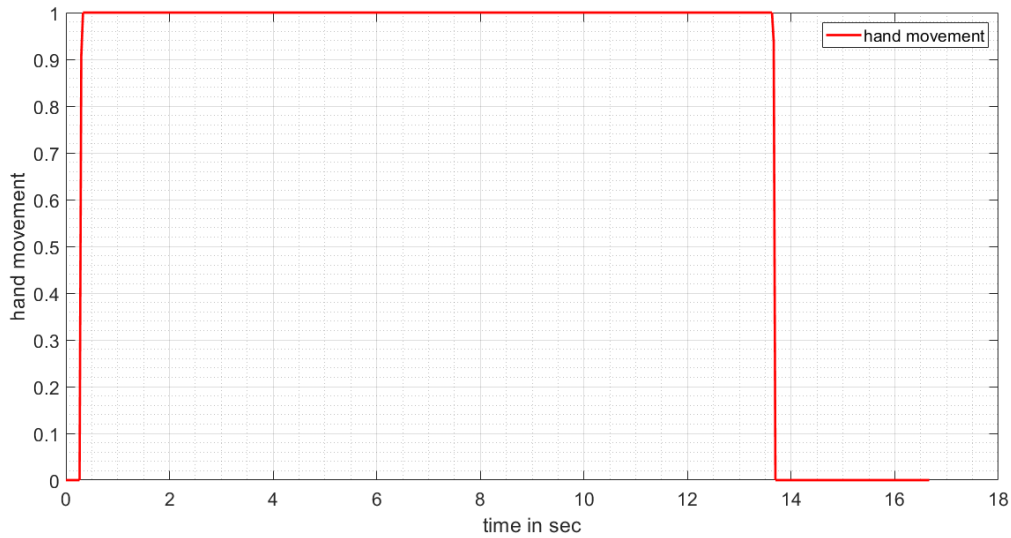


Figure 5.40: “0” corresponds to hand "steady "condition, “1” to hand "moving "condition.

From this graph (figure 5.40) the following parameters have been extracted (as described in section 5.10):

- ✓ *Test Duration*
- ✓ The rate (number of pegs inserted / test duration)
- ✓

5.9 The graph “BB overlapping”

The graph “BB overlapping” allows to understand when the board is free of occlusions due to the hand or it is not. During the occlusion free periods the number of empty holes on the board is evaluated). This graph was obtained by the overlapping procedure of the bounding boxes (hand and board) described in the section 5.6.

The graph “BB overlapping” is shown in the figure 5.41

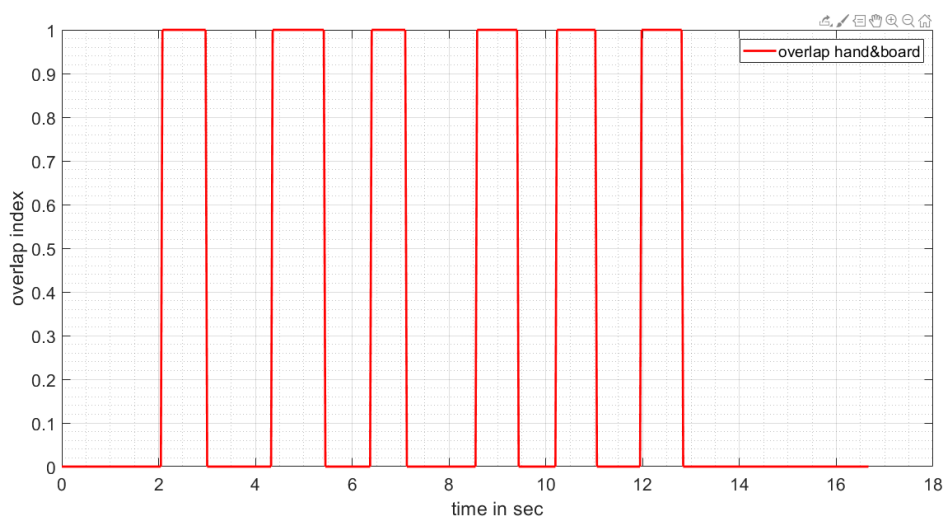


Figure 5.41: “0” corresponds to the non-overlap condition (board occlusion) of hand and board, “1” corresponds to the overlap condition of hand and board

From the graph of figure 5.41 the following parameters have been extracted as described in section 5.10:

- ✓ Time taken to insert the first peg.
- ✓ The duration of the single period at "1": overlap between hand and board (time taken to insert the pegs)
- ✓ The mean value and the standard deviation were calculated over all the periods that have a value equal to 1.
- ✓ The duration of the single period at "0": non-overlap between hand and board (time taken to take the pegs from the table)
- ✓ The mean value and the standard deviation were calculated over all the periods that have a value equal to 0.
- ✓

5.10 Motion Analysis Results: Kinematic Parameters

As a result of the overall analysis procedure, a set of kinematic parameters have been extracted from the trajectories and graphs previously described. The aim is to objectively characterize the motor performance by the means of physical quantities that can be measured and compared over time. The kinematic parameters should convey further information able to better support the standard clinical evaluation, which is generally limited only to consider only the number of pegs inserted during the test duration. The parameters extracted from trajectories and graphs used to better characterize the motor performance are the following ones:

- ❖ ***Time taken to insert the first peg (TFP)***: this parameter allows, for example, to detect a difficulty in starting the hand movement with respect to the beginning of the test: higher values may indicate a longer reaction time and therefore greater difficulty. This parameter is expressed in seconds.
- ❖ ***Duration of periods "1" (DP_ON)***: this information allows to quantify the difficulty in inserting the pegs into the board (longer durations: means that hand is kept for longer on the board), and the smooth execution of the exercise (for example, decrease in performance due to fatigue). The mean (DP_{ON_m}) and the standard deviation ($DP_{ON_{SD}}$) of the former parameters are also provided. They represent an indication of variability in duration (greater values corresponds to greater variability of the durations and consequently indicates irregularity in motor performance). These parameters are expressed in seconds.
- ❖ ***Duration of periods "0" (DP_OFF)***: this parameter allows to detect greater difficulty in retrieving the pegs from the table (longer duration: the hand takes longer to retrieve the pegs) and a slacken execution of the exercise (decrease in performance due to fatigue). The mean

(DP_OFF_m) and the standard deviation (DP_OFF_{SD}) are also provided, which represents an indication on duration variability (the greater values correspond to greater variability of the durations and consequently indicates irregularity in motor performance). These parameters are expressed in seconds.

- ❖ **Test Duration (TD):** this parameter allows to estimate the actual duration of the exercise (time spent between the starting and ending times, which is automatically detected). Combined with the number of pegs, this parameter gives a general indication of motor performance as corresponding to the standard clinical evaluation. A patient with less difficulty will probably finish the test before the maximum time established by the experimental protocol (50 seconds) by inserting all the pegs into the board; a patient with more difficulty will take longer to insert all the pegs, running out of time and failing to complete the test in the expected maximum time. This parameter is expressed in seconds
- ❖ **Number of pegs (NoP):** number of inserted pegs calculated from the number of holes detected on the board at the end of the test.
- ❖ **Rate (RT):** This parameter represents a measure of the speed in performing the test. The lower the RT value, the lower the speed of inserting the pegs, indicating greater difficulty in completing the test. This parameter is expressed in number of pegs inserted/ test duration.
- ❖ **Quantity of Hand Movement (QHM):** this parameter represents the total distance travelled by the hand during the exercise. It is obtained from the 3D trajectory of the hand with respect to the initial position. This parameter is expressed in mm.

It is important to note that these parameters provide much more detailed information on motor performance than just the number of pegs inserted at the end of NHPT, allowing for easy comparison of motor performance over time (e.g. comparing parameters at the start and end of a rehabilitation program to evaluate functional recovery of the hemiparetic limb).

These kinematic parameters were extracted on some experimental video sequences acquired on healthy subjects, using both the RGB and HSV color space-based hand tracking model.

The following tables (5.6 and 5.7) show an example of kinematic parameters extracted for the motor performance of one of the healthy subjects examined. As can be seen, the values of parameters using the two tracking algorithms (RGB and HSV) are very similar, confirming what was qualitatively deduced from the graphs of the 2D and 3D trajectories.

Parameter Name	<i>Parameter value</i>					
TFP (sec)	2.079					
DP_ON (sec)	0.924	1.089	0.726	0.858	0.825	0.825
DP_OFF (sec)	1.353	0.957	1.452	0.792	0.924	
$DP_ON_m(sec)$	0.880					
$DP_OFF_m(sec)$	1.095					
$DP_ON_{SD}(sec)$	0.121					
$DP_OFF_{SD}(sec)$	0.289					
TD(sec)	13.398					
RT (pegs/sec)	0.447					
NoP	6					
QHM (mm)	1461.3					

Table 5.6: Kinematic Parameters for tracking algorithm in HSV color space

Parameter Name	<i>Parameter Value</i>					
TFP (sec)	2.013					
DP_ON (sec)	0.990	1.089	0.759	0.858	0.825	0.858
DP_OFF (sec)	1.353	0.957	1.419	0.792	0.924	
$DP_ON_m(sec)$	0.896					
$DP_OFF_m(sec)$	1.089					
$DP_ON_{SD}(sec)$	0.120					
$DP_OFF_{SD}(sec)$	0.279					
TD (sec)	13.365					
RT (pegs/sec)	0.448					
NoP	6					
QHM (mm)	1454.1					

Table 5.7: Kinematic Parameters in RGB color space

The Test Duration (TD) parameter was extracted from the graph shown in figure 5.40, the calculation of this parameter was described in section 5.9.

As described in section 5.6, the MATLAB function **bbxOverlapRatio** was used to evaluate the overlap between bounding boxes. The overlapRatio vector returned by this MATLAB function was used to calculate the duration of the overlapping/non-overlapping periods (which are equal to 1 and 0 as shown in the graph “BB overlapping” (figure 5.38)). In particular DP_OF is the difference between the instant of time in which the vector overlapRatio passes from a value less than 1 to 0 and the instant of time in which overlapRatio passes from 0 to a value less than 1.

While DP_ON is the difference between the instant of time in which the vector overlapRatio passes from 0 to a value less than 1 and the instant of time in which overlapRatio passes from a value less than 1 to 0.

TFP is calculated as the duration in which the vector overlapRatio passes for the first time from 0 to a value less than 1.

QHM is the sum of all the variations between one point and another, it represents how far the hand was moved overall during the whole exercise.

CHAPTER 6

Case Study: Application to Post-Stroke subjects

6.1 Introduction

The goal of this chapter is to apply the developed procedure to post-strokes subjects to highlight possible problems that may arise in the analysis of motor performance of subjects with motor disabilities. This chapter refers to a set of preliminary tests performed before the motor rehabilitation treatment on same post-stroke subjects with hemiparesis on one arm. The NHPT experimental clinical protocol provides for a maximum test duration of 50 seconds in which subjects must insert all 9 pegs on the board.

The operator can decide to stop the exercise before the expected time in two conditions:

- ❖ The test is completed by the positioning of the 9 pegs correctly before 50 seconds.
- ❖ An excessive fatigue is observed.

The video sequences were collected using the acquisition system, and then analysed with the procedure developed. The main goal is to verify if the kinematic parameters are able to detect anomalies in motor performance of post-stroke subjects and differences with respect to motor performance of healthy subjects.

Among the several video sequences analysed, problems and results will be reported on the video sequence related to the subject EMI3, a subject with hemiparesis falling in an excessive fatigue condition, with a final score of 2 pegs inserted in about 20 seconds.

In this chapter I will describe the issues that were highlighted when the script was used on video sequences of post-stroke subjects. The main problems that emerged are partly due to the experimental protocol, which requires the scrupulous observance of specific requirements, and partly to the difficult to control the movements of stroke affected subjects compared to healthy subjects which can represent a criticality for the tracking algorithm. The analysis of the video sequence of subject EMI3 is reported as an example.

6.2 Color Thresholds issue

The color thresholds for Color Segmentation of hand and board were changed because the ambient light, when EMI3 subject performed the NHPT, was different compared to previous conditions. In particular, the minimum thresholds used to isolate the board was changed because the EMI3 was

performed in darker condition than the previous tests. Hence, by using the thresholds described in the previous chapter, many "darker" areas were not considered as part of the board, creating problems in the detection of holes on board. This is a typical situation in uncontrolled environments: other than a manual adaptation of thresholds as in this case, an automatic procedure of color calibration needs to be implemented in the perspective of using this approach of remote monitoring of patients at-home, when it is impossible to set ambient light conditions.

	R(red)		G(green)		B(blue)	
	Minimum Threshold	Maximum Threshold	Minimum Threshold	Maximum Threshold	Minimum Threshold	Maximum Threshold
Hand	20.000	65.000	20.000	65.000	20.000	65.000
Board	115.000	170.000	80.000	130.000	50.000	90.000

Table 6.1: The thresholds set in the RGB color space

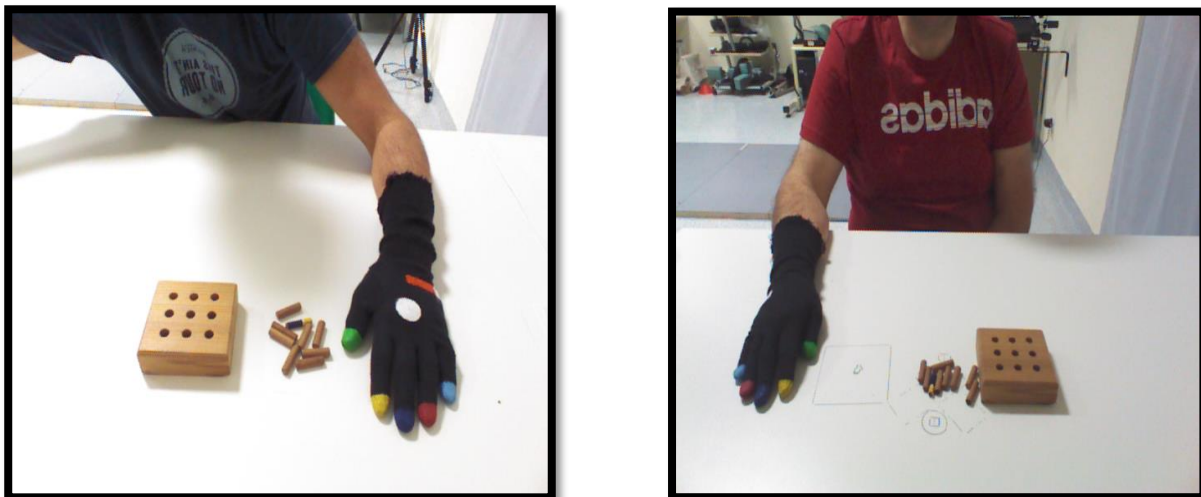


Figure 6.1: Two tests performed in different ambient lighting conditions

6.3 Board Tracking problem

As described in section 5.2, the color blobs that satisfy color threshold could be found everywhere in the scene observed by the optical device. In this video sequence, for example, the color of patient's arm and board were similar due to the light conditions and both satisfy the color thresholds defined for the board. For this reason, the area of patient's arm was sometimes confused by the board tracking algorithm (largest color blob on patient's arm) causing failures in the detection of holes (Figure 6.2). To overcome this problem, the segmentation Depth and the bb_mask described in section 5.2 was used also to define an area of interest reducing the area of the RGB image in which the board tracking algorithm was applied (Figure 6.3).

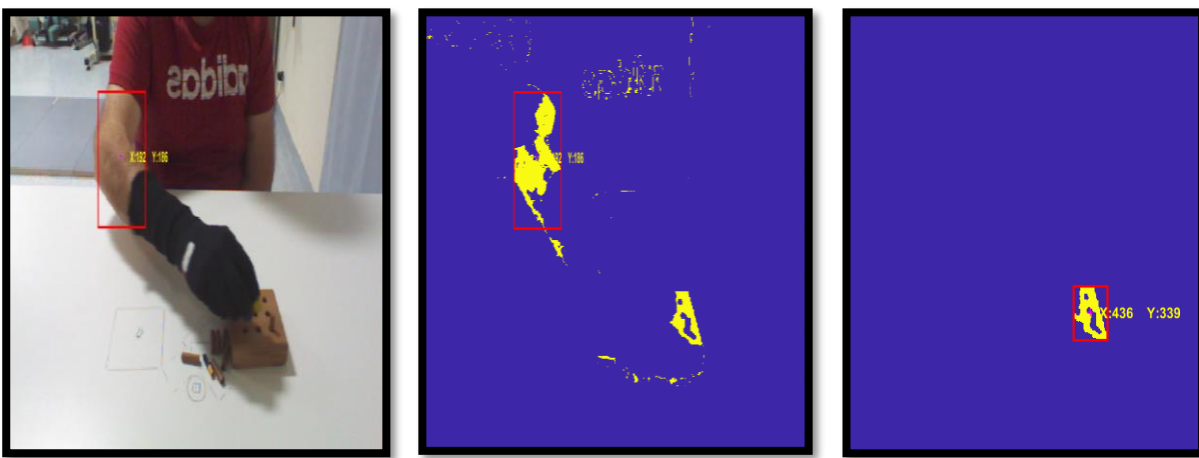


Figure 6.2:Left: the area of patient's arm was confused by the board tracking algorithm; Center: image mask; Right: the final image mask obtained.

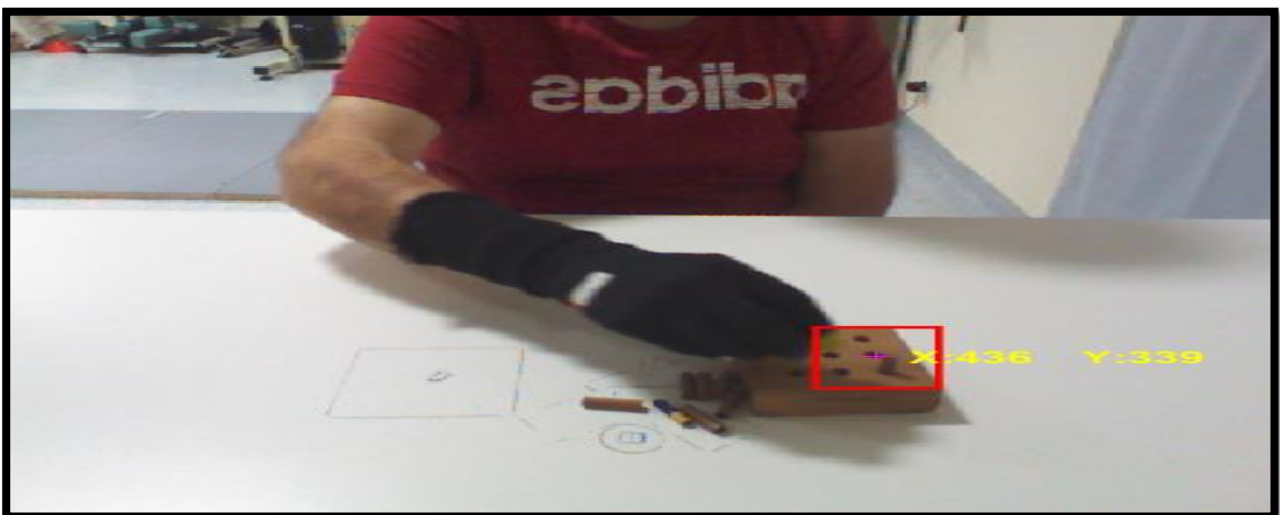


Figure 6.3 : Final result obtained: the board was detected correctly by the board tracking algorithm

6.4 Shadow of the hand on the board

When the hand approached the board for the insertion of the peg, the shadow of the hand could be created on the board causing problems to the overlap function described in the previous chapter, because a part of the board may not be correctly identified by applying the defined thresholds for the board (Figure 6.5), due to the shadow that makes it “darker”. This problem was highlighted for the video sequence of EIM3 subject, probably in correlation to the particular light conditions

The problem was overcome by not applying the algorithm for the detection of circles (and therefore holes) when the shadow hand is detected on the board, treating this condition as a sort of overlap between the two bounding boxes.

The method used is the following: In this case, the algorithm change concerns the percentage of pixels that meet the color thresholds for the board: The number of pixels of the first frame (where the board is free) was considered as the maximum (Figure 6.4); in the following frames the number of pixels that satisfy the thresholds was calculated: obviously the number of pixels decreased in the case of shadow on the board precisely because the darker areas will no longer satisfy the pre-set thresholds. This condition was exploited to avoid applying the circle detection algorithm (Figure 6.4).

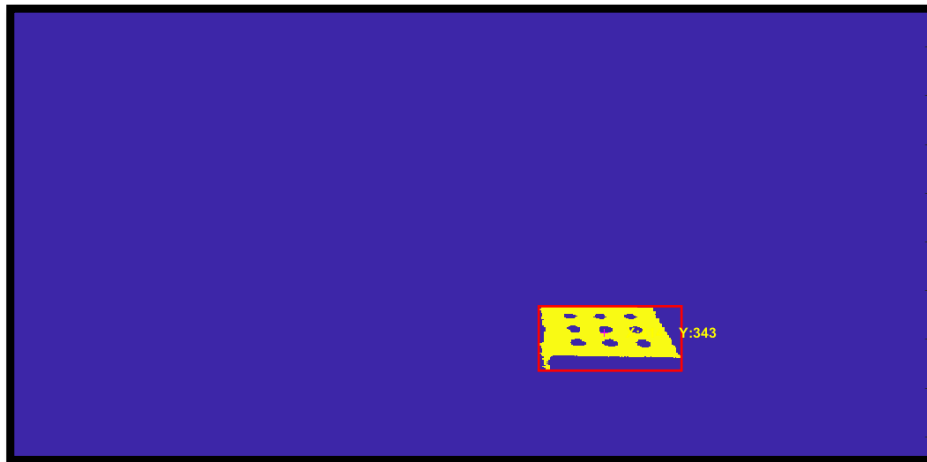


Figure 6.4: Image mask of first frame

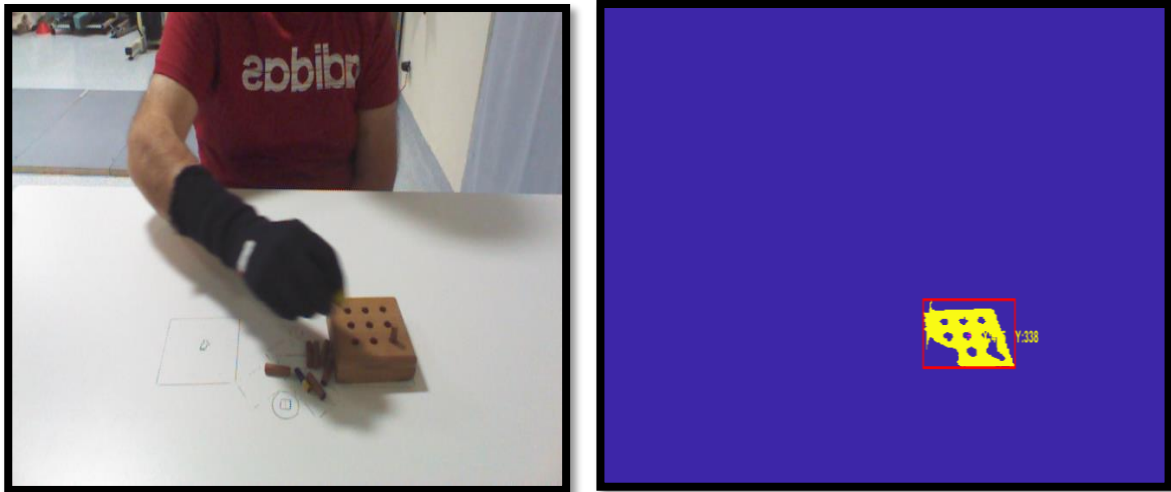


Figure 6.5: The effect of the shadow of the hand on the image mask

6.5 Motion analysis results: Trajectories and graphics

The objective of this paragraph is to present and discuss the results obtained from the analysis of the NHPT performed by the EMI3 subject, after modifying the analysis procedure as described in the previous sections to address the highlighted problems. The same methods described in in the previous chapter was used to obtain trajectories and graphics. For this sequence I have reported only the results obtained on the RGB space since similar results have been obtained on the HSV space as already highlighted in the previous chapter.

6.5.1 The trajectory of the hand in 2D space

The same procedure described in section 5.8.1 was used to obtain the 2D trajectory of the hand during the test performed by post stroke subject EMI3 subject.

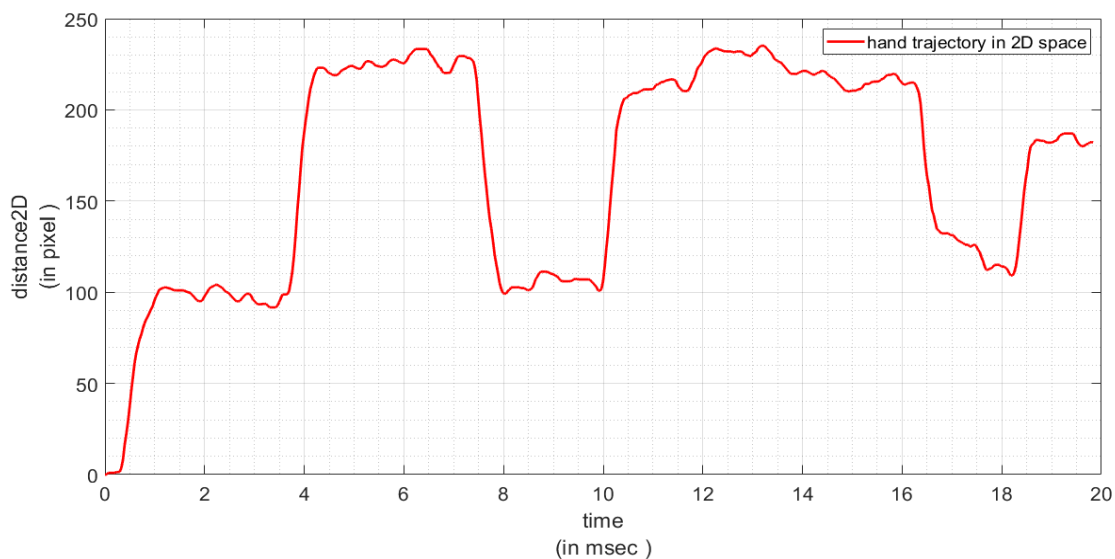


Figure 6.6: Trajectory of the hand in 2D space (in RGB color space) vs. the time (in s).

From the graphical analysis of the figure 6.6, it should be noted that the time taken by patient EMI3 to insert a single peg was greater than the time taken by a normal subject (Figure 5.36), highlighting greater difficulty in complete the task. It is therefore clear that the trajectory of the hand movement, captured by the acquisition system, provides a qualitative indicating of the motor performance from which it is possible to extract kinematic measures capable of discriminating the two-motor performance.

6.5.2 The trajectory of the hand in 3D space

The trajectory of the hand in 2D space was then transformed into 3D space, as shown in the Figure 6.7.

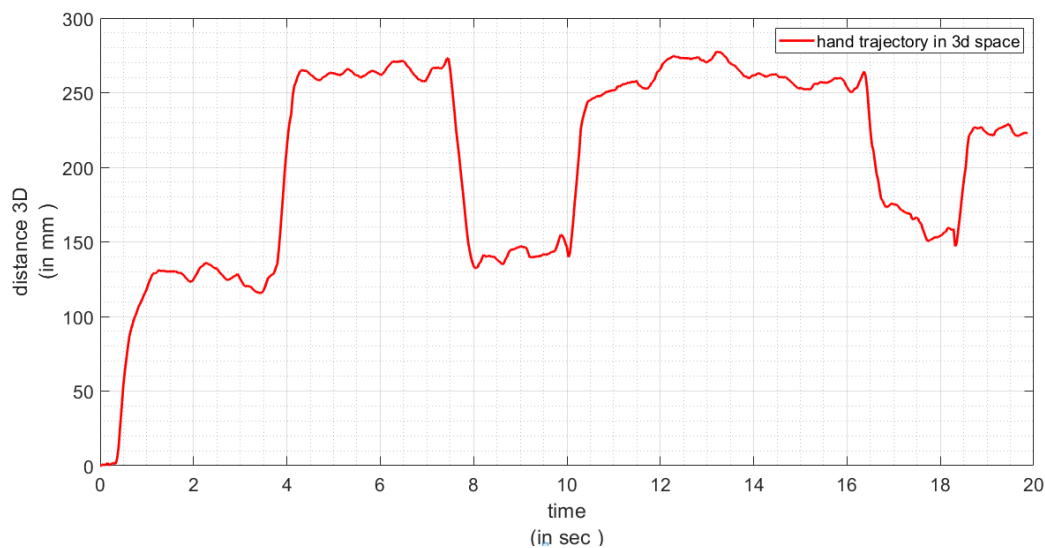


Figure 6.7: Trajectory of the hand in 3D space vs time, in RGB color space

The 3D trajectory highlights also a sort of instability or irregularity, both during the positioning of the pegs and in the retrieval of the pegs from table. This could be due to greater impairment in fine handing of small objects (such as pegs) and the continuous adjustment movement to correctly position pegs in holes.

6.5.3 The graph of the holes detected

The correctly number of holes was detected, as shown in figure 6.8.

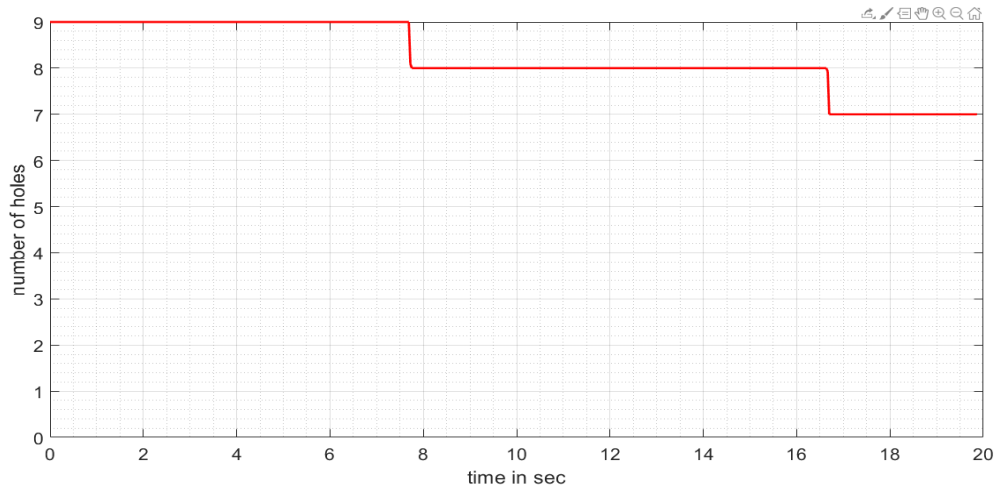


Figure 6.8: Correct number of holes detected on the board, versus time

In this case, the final number of pegs inserted by patient EMI3 was two pegs because the NHPT was interrupted in advance by the operator.

6.5.4 The graph " hand in Movement"

The graph "hand in movement" was created as shown in figure 6.9

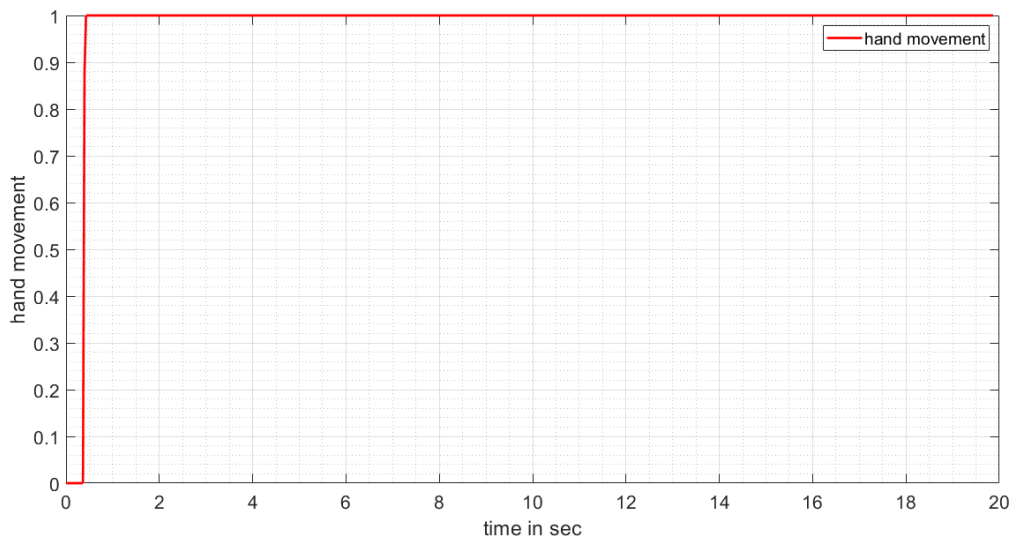


Figure 6.9: "0" : "steady hand"; "1": "moving hand".

In this case, the operator decided to stop the acquisition in advance because the patient EIM3 was having difficulty in moving his arm.

6.5.5 The graph “BB overlapping”

The graph “hand in movement” was created as shown in the figure 6.10.

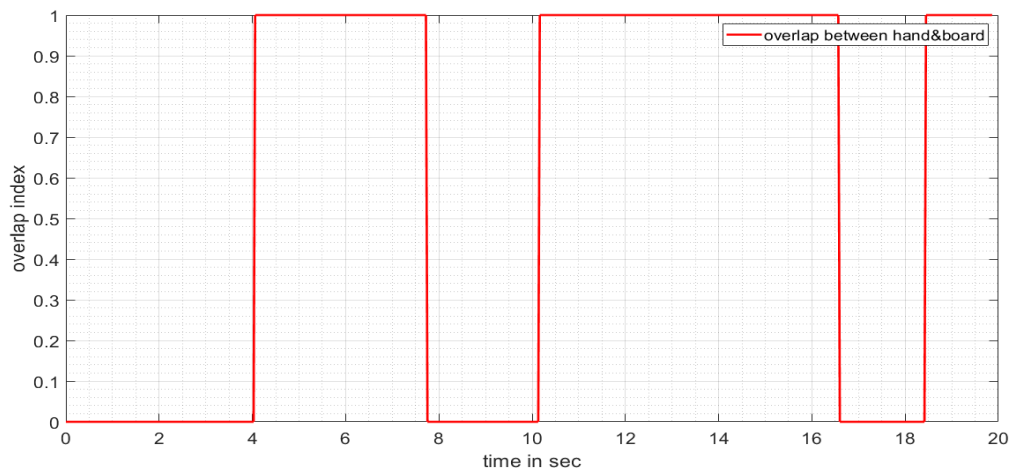


Figure 6.10:“0”: no-overlap between hand and board; “1”: overlap between hand and board

In this case, a significant difference was noted between the graph “BB overlapping” in figure 6.9 and the graph “BB overlapping” in figure 5.41. It is clear that the overlap time between the board and the hand was greater in the case of the EMI3 patient.

The EMI3 patient takes a long time to position the peg correctly due to the motor impairment of the hemiparetic limb, and the time that passes from the start of the test to the insertion of the first peg is also longer than in the case of the normal subject, this is indicative of greater motor difficulty.

6.6 Motion Analysis Results: Kinematic Parameters

Tables 6.2 shows the numerical values of the parameters extracted from the graph “BB overlapping” described in section 6.5.5. The same procedure described in in the previous chapter was used to obtain the following parameters.

Parameter Name	Parameter Value	
TFP (s)	4.0590	
DP_ON (s)	3.6960	6.4350
DP_OFF (s)	2.4090	1.8480
$DP_ON_m(s)$	5.0655	
$DP_OFF_m(s)$	2.1285	
$DP_ON_{SD}(s)$	1.9368	
$DP_OFF_{SD}(s)$	2.1285	
TD(s)	19.4700	
NoP	2	
RT (pegs/sec)	0.102	
QHM (mm)	1124.3	

Table 6.2.: Kinematic Parameters in RGB color space

When the kinematic parameters in Tables 6.1 and 5.4 were compared, it was clear that the patient EMI3 had more difficulty picking up pegs into board and he was very slow compared to a healthy subject.

The test duration was extracted from the graph shown in figure 6.8. As expected, the healthy subject demonstrated the highest performance (highest rate), and the patient EMI3 demonstrated the lowest performance (lowest rate), as it is evident from the parameter values of tables 6.2 and 5.7.

TFP indicates that EMI3 subject takes longer to insert the first pegs into board. The longer DP_ON and DP_OFF times compared to the healthy subject objectively indicate that EMI3 subject takes longer both to insert the pegs and to retrieve them from the board, an indication also confirmed by the respective average values $DP_ON_m(s)$ and $DP_OFF_m(s)$.

The parameters relating to the standard deviation also show a certain irregularity in the movements, probably due to fatigue in carrying out the task, which led the operator to prematurely interrupt the test. The RT parameter indicates that the test was performed rather slowly compared to the case of the healthy subject. From the analysis of the QHM parameter it might seem that the EMI3 subject has performed less hand movement in total than the healthy subject, but if this value is compared to the

number of final pegs inserted, it is clear that the EMI3 subject has made more hand movements of his own due to his difficulty in the insertion and retrieval phases of the pegs. All this information can therefore objectively confirm what emerged from the graphic and qualitative analysis of the movement trajectories, thus denoting a worse performance for the EMI3 subject characterized by an evident motor impairment.

The analysis of motor performance through the defined kinematic parameters therefore seems to offer the possibility of a more complete clinical evaluation that would otherwise not emerge from the traditional clinical evaluation which would be limited to crude scores "6 pegs / 13.4 seconds" for the healthy subject and "2 pegs. / 19.5 seconds" in the case of the EMI3 subject.

This implies the possibility of obtaining an objective and complete measure of motor performance and also of being able to objectively compare different motor performance related to the same subjects, for example at the start and at the end of a rehabilitation program. This approach is applicable both in the clinical setting, but also in the home setting for the remote evaluation of the motor functions.

Chapter 7

Conclusion

The purpose of this thesis work was to realize an automatic analysis and evaluation of the Nine Hole Peg Test (NHPT), a clinical test commonly used to assess the hand motor function in post-stroke subjects. A vision-based system, using an RGB-Depth sensor and colored gloves, was used for the acquisition of video sequences of healthy controls and subjects with hemiparesis during the execution of the NHPT. A dedicated software, based on Computer Vision approach, was developed for the analysis of the NHPT video sequences. In particular, this software aims to evaluate and characterize the motor performance by means of a set of kinematic parameters extracted from the trajectories of the movements captured by the acquisition system. A hand tracking algorithm has been developed to automatically detect and track the 2D and 3D movements of the hand with black glove, using both the synchronized information of color and depth videos provided by the RGB-Depth sensor. A board tracking algorithm has been developed to automatically detect and track the position of the test board. The hand tracking algorithm implements a Color Segmentation technique, using estimated color thresholds to isolate the color blob of the hand in each frame of the video sequence and to obtain movement trajectories from which it is possible to extract the kinematic parameters characterizing the test performance. The board tracking algorithm implements a Color Segmentation technique, using estimated color thresholds to isolate the color blob of the finger hand in each frame of the video sequence and to estimate the region of interest (bounding box) in which is evaluated the number of pegs correctly positioned. Two color spaces, RGB and HSV, were considered to realize the tracking algorithms, in particular because HSV should be more robust to changes in ambient light conditions and it could be the better choice in uncontrolled environments as, for example, home environment. Other Computer Vision techniques were used to make the tracking algorithms robust (depth segmentation, morphological filters, overlapping procedure) and to evaluate the number of pegs correctly inserted into the board (Holes Detection, Hough transform for circle detection, removal of duplicate circles). Several graphs were used to provide an immediate qualitative indication about the motor performance that was then confirmed by the objective kinematic parameters estimated: graphs and parameters may support the clinical assessment of the NHPT that, in the standard test, is limited to the number of pegs inserted and test duration without reporting any other information about the

performance. A set of kinematic parameters characterizing the performance were estimated both for healthy and post-stroke subjects.

The preliminary results show that the defined kinematic parameters are able to detect differences between the motor performance of healthy and subjects with mild post stroke side effects in the execution of NHPT: the acquisition system is so able to capture features of the movements that the analysis procedure can automatically evaluate through objective measures.

These results are therefore encouraging, allowing us to hypothesize that the defined kinematic parameters could support the automated clinical assessment through a movement analysis procedure capable of objectively capturing and measuring more specific aspects of motor function and impairment. This is important in particular for comparing different motor performance and for quantifying improvements or worsening over time. In addition, the use of vision systems and optical devices makes this approach easy to use and, in particular, non-invasive for patients with disabilities in the perspective of home monitoring.

Certainly, the results need to be confirmed by other studies. Future researches, for example, should validate the 2D/3D measurements obtained with respect to standard reference systems (i.e., optoelectronic systems) for movement analysis and also verify the ability of the defined parameters in the automatic detection of improvements in motor performance following rehabilitation treatments. A weakness of this approach, typical when optical devices are used, is related to ambient light, which is particularly critical in uncontrolled environments. The analysis of video sequences made at different times and environments highlighted this problem, requiring a manual adjustment of the color thresholds used by the detection and tracking algorithms. A further improvement to the analysis procedure will be the implementation of an automatic calibration procedure of the algorithms based on the detected light conditions.

However, once the algorithms and the results have been consolidated, this objective and automatic assessment of motor performance in NHPT can be easily used for applications of remote monitoring and rehabilitation in home environments.

Bibliography

- [1] M. A. M. B. e. a. Jane Burridge, "A Systematic Review of International Clinical Guidelines for Rehabilitation of People With Neurological Conditions: What Recommendations Are Made for Upper Limb Assessment?," *Frontiers ;Front. Neurol.*, 25 June 2019 | <https://doi.org/10.3389/fneur.2019.00567>, 2019.
- [2] W. H. Organization, "The Atlas of Heart Diseases and Stroke," [Online]. Available: https://www.who.int/cardiovascular_diseases/resources/atlas/en/.
- [3] ministro della salute ,ictus, [Online]. Available: http://www.salute.gov.it/portale/salute/p1_5.jsp?lingua=italiano&id=28&area=Malattie_cardiovascolari.
- [4] "Italian Stroke Organization, Ictus cerebrale: linee guida italiane di prevenzione e trattamento Raccomandazioni e Sintesi," <https://www.iso-stroke.it/wp-content/uploads/2017/02/LIBRO-SPREAD-VIII-ED-13-09-16.pdf>.
- [5] Stroke Alliance for Europe, "The Burden of Stroke in Europe" <https://www.stroke.org.uk/>.
- [6] "World Health Organisation. Cerebrovascular Disorders: a clinical and research classification," [Online]. Available: http://whqlibdoc.who.int/offset/WHO_OFFSET_43.pdf. [Accessed 1 september 2020].
- [7] *L. Monfils, "CT-scan of the brain with a RIGHT MCA infarct," ,.wikimedia Commons, 21 July 2008.*
- [8] *J. Heilman, "A intra parenchymal bleed with surrounding edema", wikipedia29August 2011..*
- [9] *Judy Haluka, ACLS trainig center ,https://www.acls.net/acls-suspected-stroke-algorithm.htm, accessed 30 september 2020.*
- [10] *S. Vietta and F. M. e. al, "Sempione News," 15 Settembre 2017. [Online]. Available: https://www.sempionenews.it/territorio/come-prevenire-ictus/. [Accessed august 2020]..*
- [11] *"Broks Rehabilitation," Mar 10, 2015. [Online]. Available: https://brooksrehab.org/blog/stroke-patient-sean-bretz-comes-full-circle-in-his-recovery/. [Accessed August 2020]..*
- [12] J. L. Saver, Time Is Brain-Quantified, *Stroke*, . 2006;37:263–266 <https://doi.org/10.1161/01.STR.0000196957.55928.ab>.

- [13] A. K. Boehme et al., Stroke Risk Factors, Genetics, and Prevention, *Circ Res.* 2017 February 03; 120(3): 472–495. doi:10.1161/CIRCRESAHA.116.308398.
- [14] Hypertension: facts and definitions, <https://www.who.int/news-room/fact-sheets/detail/hypertension>.
- [15] Tocci, G., et al., Blood pressure levels and control in Italy: comprehensive analysis of clinical data from 2000-2005 and 2005-2011 hypertension surveys. *J Hum Hypertens*, 2015. 29(11): p. 696-701.
- [16] Sarwar N. et al., Diabetes mellitus, fasting blood glucose concentration, and risk of vascular disease: a collaborative meta-analysis of 102 prospective studies. *Emerging Risk Factors Collaboration, Lancet.* 2010; 26;375:2215-2222.
- [17] World Health Organization, Diabetes: key facts, <https://www.who.int/news-room/fact-sheets/detail/diabetes>.
- [18] Y. Zhang, et al. "Total and high-density lipoprotein cholesterol and stroke risk." *Stroke* 43.7 (2012): 1768-1774..
- [19] "World Health Organization, Prevalence of tobacco smoking," World Health Organization, Prevalence of tobacco smoking, <https://www.who.int/gho/tobacco/use/en/>.
- [20] Feinberg W.M. et al., Prevalence, age distribution and gender of patients with atrial fibrillation, *Arch. Intern. Med.* 1995; 155: 469-473.
- [21] J. Burridge et al., A Systematic Review of International Clinical Guidelines for Rehabilitation of People With Neurological Conditions: What Recommendations Are Made for Upper Limb Assessment?, *Front. Neurol.*, 25 June 2019 | <https://doi.org/10.3389/>.
- [22] Liu, Jia, et al. "Augmented reality-based training system for hand rehabilitation." *Multimedia Tools and Applications* 76.13 (2017): 14847-14867..
- [23] *John Greim, "WebMD, Slideshow: Stroke Rehab to Regain Arm Movement," on April 18, 2019, 18 April 2019. [Online]. Available: https://www.webmd.com/stroke/ss/slideshow-stroke. [Accessed august 2020].*
- [24] *Gomes, C.L.A., Cacho, R.O., Nobrega, V.T.B. et al. Low-cost equipment for the evaluation of reach and grasp in post-stroke individuals: a pilot study. BioMed Eng OnLine 19, 14 (2020). https://doi.org/10.1186/s12938-020-0758-7.*
- [25] Simpson, Lisa A., et al. "Rating of Everyday Arm-Use in the Community and Home (REACH) scale for capturing affected arm-use after stroke: development, reliability, and validity." *PLoS One* 8.12 (2013): e83405..
- [26] Oña E.D., et al., The Automated Box and Blocks Test an Autonomous Assessment Method of Gross Manual Dexterity in Stroke Rehabilitation. (2017), In: Gao Y., Fallah S., Jin Y., Lekakou C. (eds)

Towards Autonomous Robotic Systems. TAROS 2017. Lecture Notes, Notes in Computer Science, vol 10454. Springer, Cham. https://doi.org/10.1007/978-3-319-64107-2_9 .

- [27] R. Nijland, et al. "A comparison of two validated tests for upper limb function after stroke: The Wolf Motor Function Test and the Action Research Arm Test." *Journal of rehabilitation medicine* 42.7 (2010): 694-696..
- [28] Spilker, Judith, et al. "Using the NIH Stroke Scale to assess stroke patients." *Journal of Neuroscience Nursing* 29.6 (1997): 384-393..
- [29] C. Weimar C, et al., "Age and national institutes of health stroke scale score within 6 hours after onset are accurate predictors of outcome after cerebral ischemia", *Stroke*, 2004, 35 (1): 158–162. doi:10.1161/01.str.0000106761.94985.8b. PMID 1468477.
- [30] *Glymour M, Berkman L, Ertel K, Fay M, Glass T, Furie K (2007). "Lesion characteristics, NIH Stroke Scale, and functional recovery after stroke". American Journal of Physical Medicine & Rehabilitation. 86 (9): 725–733. doi:10.1097/phm.0b013e31813e0a32.*
- [31] Yu, Jaehak, et al. "An Elderly Health Monitoring System Using Machine Learning and In-Depth Analysis Techniques on the NIH Stroke Scale." *Mathematics* 8.7 (2020): 1115..
- [32] G. M.Johansson, "Measurement properties of the motor evaluation scale for upper extremity in stroke patients (MESUPES)." *Disability and rehabilitation* 34.4 (2012): 288-294.
- [33] MOTOR EVALUATION SCALE FOR UPPER EXTREMITY IN STROKE PATIENTS (MESUPES), <https://www.strokengine.ca/en/indepth/mesupes/>.
- [34] V. Mathiowetzl, et al. "Adult norms for the nine hole peg test of finger dexterity." *The Occupational Therapy Journal of Research* 5.1 (1985): 24-38..
- [35] Van de Winckel, H. Feys, et al., Can quality of movement be measured? Rasch analysis and inter-rater reliability of the Motor Evaluation Scale for Upper Extremity in Stroke Patients (MESUPES). *Clin Rehabil*, 20(10), 2006, 2006 Oct;20(10):871-84..
- [36] *health and care.co.uk. [Online]https://www.healthandcare.co.uk/sensation/9-hole-peg-test-for-dexterity-testing.html*, accessed 30 september 2020.
- [37] "SPINPOI," Heinemann, A. (2010). *Rehabilitation Measures Database. Rehabilitation Institute of Chicago, Center for Rehabilitation Outcomes Research, Northwestern University Feinberg School of Medicine, Department of Medical Social Sciences Informatics Gro, Informatics Group*. Retrieval, [Online]. Available: <http://www.spinpoi.com/the-pre-tests/>..
- [38] Silva LC. Nine-hole peg test for evaluation of hand function: The advantages and shortcomings. *Neurol India* [serial online] 2017 [cited 2020 Jun 30];65:1033-4. Available from: <http://www.neurologyindia.com/text.asp?2017/65/5/1033/214081>.

- [39] Johansson, Gudrun M., and Charlotte K. Häger. "A modified standardized nine hole peg test for valid and reliable kinematic assessment of dexterity post-stroke." *Journal of NeuroEngineering and Rehabilitation* 16.1 (2019): 8..
- [40] A. Jana, "Abhijit's Blog," 14 september 2011. [Online]. Available: <https://abhijitjana.net/2011/09/14/development-with-kinect-net-sdk-part-i-installation-and-development-environment-setup/>. [Accessed 3 september 2020].
- [41] Ferraris C, Nerino R, Chimienti A, et al. A Self-Managed System for Automated Assessment of UPDRS Upper Limb Tasks in Parkinson's Disease. *Sensors (Basel)*. 2018;18(10):3523. Published 2018 Oct 18. doi:10.3390/s18103523.
- [42] P. Sebastian, Y. Vooi and R. Comly, "The Effect of Colour Space on Tracking Robustness," *Universiti Teknologi PETRONAS*, pp. 1-2, Downloaded on October 13, 2008 at 04:24 from IEEE Xplore. Restrictions apply..

